

PERFORMANCE INVESTIGATION OF A CSI BASED POWER LINE CONDITIONER WITH ANN CONTROL

A DISSERTATION

*Submitted in partial fulfillment of the
requirements for the award of the degree
of*

MASTER OF TECHNOLOGY

in

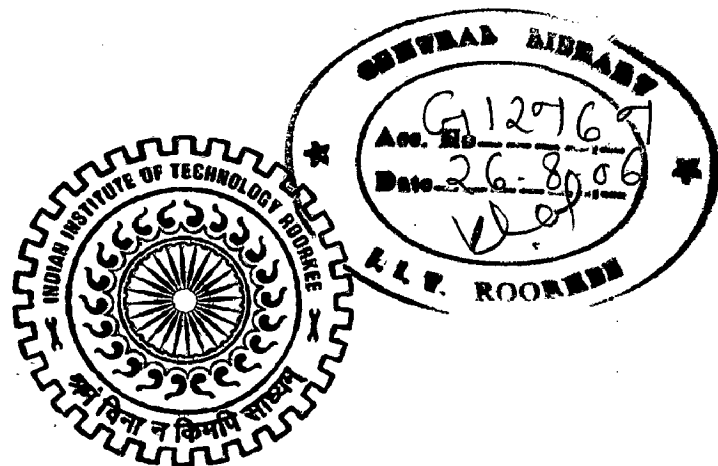
ELECTRICAL ENGINEERING

(With Specialization in Power Apparatus and Electric Drives)

By

SANDIP KUMAR CHATTERJEE

IP



**DEPARTMENT OF ELECTRICAL ENGINEERING
INDIAN INSTITUTE OF TECHNOLOGY ROORKEE
ROORKEE-247 667 (INDIA)**

JUNE, 2006

Candidate's Declaration

I here by declare that the work which is being presented in the Dissertation Thesis entitled "**Performance Investigation of a CSI based Power Line Conditioner with ANN Control**" in partial fulfillment of the requirements for the award of the degree **Master of Technology in Electrical Engineering** with specialization in **Power Apparatus and Electric Drives**, submitted in the **Department of Electrical Engineering, Indian Institute of Technology, Roorkee, India - 247 667**. This is an authentic record of my own work carried out in the period of last two semesters from Aug 2005 to May 2006, under the supervision of **Dr. Pramod Agarwal**, Professor, and **Dr. G.N. Pillai**, Assistant Professor, Department of Electrical Engineering, Indian Institute of Technology, Roorkee, INDIA - 247 667.


The matter embodied in this Dissertation Thesis has not been submitted by me for the award of any other degree or diploma.

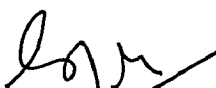
Date: 29.06.06.

Place: Roorkee


(Sandip Kumar Chatterjee)

This is to certify that the above statements made by the candidate are correct to the best of my knowledge.


(Dr. Pramod Agarwal)
Professor,
Dept. of Electrical Engineering,
Indian Institute of Technology,
Roorkee-247 667,
India.


(Dr. G.N. Pillai)
Assistant Professor,
Dept. of Electrical Engineering,
Indian Institute of Technology,
Roorkee-247 667,
India.

Acknowledgement

I wish to place on record my deep sense of gratitude and indebtedness to my guides **Dr. Pramod Agarwal**, Professor, and **Dr. G.N. Pillai**, Assistant Professor, Department of Electrical Engineering, Indian Institute of Technology Roorkee, Roorkee for their wholeheartedness and high dedication with which he involved in this work. I am grateful for hours they spent in discussing and explaining even the minute details of the work in spite of their hectic schedule of work in the department.

I am very much thankful to **Dr. S. P. Gupta**, Professor and Head, Department of Electrical Engineering, IIT Roorkee for providing me all the support and facilities during my work.

I am grateful to all my teachers of the PAED group for their suggestions and constant encouragement. I am also grateful to all Research Scholars of the PAED group for their suggestions and constant encouragement.

Timely assistance and help from the laboratory staff of Drives Lab, Stores, and Workshop is sincerely acknowledged.

I gratefully acknowledge my sincere thanks to all my family members and friends for their inspirational impetus and moral support during the course of this work. I owe everything to them.

Finally, I would like express my deepest gratitude to God for His blessings.

Abstract

Solid state control of ac power using thyristors and other semiconductor switches is widely employed to feed controlled electric power to electrical loads. These nonlinear devices inject harmonic currents in the AC system and increase overall reactive power demanded by the equivalent load. The increased severity of harmonic pollution in power networks has attracted the attention of power electronics and power system engineers to develop dynamic and adjustable solutions to the power quality problems. Such equipment, generally known as active power filters (APF's), are also called active power line conditioners (APLC's).

The simulation models of different implementation techniques for current source active power filters are developed in MATLAB Simulink and the results are presented. The hysteresis PWM control is simple, but its average switching frequency is very high and varies with load conditions so that switching patterns are uneven and random. The space vector modulation (SVM) technique, with some modifications, is implemented for Current Source APF. The Artificial Neural Network is used to customize the conventional SVM approach. The technique reduces software complexity, and computation time, and increases the accuracy of the positioning of the switching instants.

List of Figures

| Figure No | Figure Description | Page No |
|-----------|---|---------|
| Fig 1 | Shunt Active Power Filter | 11 |
| Fig 2 | Voltage Source Shunt Active Power Filter | 11 |
| Fig 3 | Current Source Shunt Active Power Filter | 12 |
| Fig 4 | Series Active Power Filter | 12 |
| Fig 5 | 3-Single phase filter topology | 15 |
| Fig 6 | Single 3-phase filter topology | 15 |
| Fig 7 | Modular Approach of Power filters | 16 |
| Fig 8 | Single Converter Approach of Power filters | 16 |
| Fig 9 | Arrangements of LC filter | 18 |
| Fig 10 | Main Circuit of CSAPF | 22 |
| Fig 11 | Simulink Model for Hysteresis controlled CSAPF | 26 |
| Fig 12 | Simulink Model for the Subsystem for the Hysteresis controller | 26 |
| Fig 13 | Simulation Results for Hysteresis Controlled CSAPF with RL load | 27 |
| Fig 14 | Simulation Results for Hysteresis Controlled CSAPF with RL load | 28 |
| Fig 15 | Simulation Results for Hysteresis Controlled CSAPF with RL load | 29 |
| Fig 16 | Simulation Results for Hysteresis Controlled CSAPF with RL load | 30 |
| Fig 17 | Simulation Results for Hysteresis Controlled CSAPF with RC load | 31 |
| Fig 18 | Simulation Results for Hysteresis Controlled CSAPF with RC load | 32 |
| Fig 19 | Simulation Results for Hysteresis Controlled CSAPF with RC load | 33 |
| Fig 20 | Space Vectors of a Voltage Source Converter | 35 |
| Fig 21 | Space Vectors of a Current Source Converter | 36 |
| Fig 22 | Current Components | 40 |
| Fig 23 | PWM patterns for CSAPF | 42 |
| Fig 24 | Simulink Model for SVM controlled CSAPF | 43 |
| Fig 25 | Simulink Model for the Subsystem for the SVM | 44 |
| Fig 26 | Simulation Results for SVM Controlled CSAPF with RL load | 44 |
| Fig 27 | Simulation Results for SVM Controlled CSAPF with RL load | 45 |
| Fig 28 | Simulation Results for SVM Controlled CSAPF with RL load | 45 |
| Fig 29 | Simulation Results for SVM Controlled CSAPF with RL load | 46 |
| Fig 30 | Simulation Results for SVM Controlled CSAPF with RL load | 47 |
| Fig 31 | Simulation Results for SVM Controlled CSAPF with RC load | 48 |
| Fig 32 | Simulation Results for SVM Controlled CSAPF with RC load | 49 |
| Fig 33 | Simplified Model of (a) Brain, (b) Neural Network | 50 |
| Fig 34 | Single Neuron Model | 51 |

| | | |
|--------|--|----|
| Fig 35 | Single Layer Perceptron | 52 |
| Fig 36 | Counter propagation Neural Networks (CPNN) | 53 |
| Fig 37 | A layer of neurons arranged in competitive layer | 55 |
| Fig 38 | Proposed SV implementation for CSAPF | 58 |
| Fig 39 | Simulink Model for ANN-SVM controlled CSAPF | 60 |
| Fig 40 | Simulink Model for the Subsystem for the ANN-SVM | 60 |
| Fig 41 | Simulation Results for ANN-SVM Controlled CSAPF with RL load | 61 |
| Fig 42 | Simulation Results for ANN-SVM Controlled CSAPF with RL load | 62 |
| Fig 43 | Simulation Results for ANN-SVM Controlled CSAPF with RL load | 63 |
| Fig 44 | Simulation Results for ANN-SVM Controlled CSAPF with RC load | 64 |
| Fig 45 | Simulation Results for ANN-SVM Controlled CSAPF with RC load | 65 |
| Fig 46 | Simulation Results for ANN-SVM Controlled CSAPF with RC load | 66 |
| Fig 47 | Dynamic performance of ANN-SVM Controlled CSAPF | 67 |
| Fig 48 | Dynamic performance of ANN-SVM Controlled CSAPF | 67 |

Contents

| | |
|--|-----------|
| <i>Candidate's Declaration</i> | i |
| <i>Acknowledgement</i> | ii |
| <i>Abstract</i> | iii |
| <i>List of Figures</i> | iv |
| <i>Contents</i> | vi |
| | |
| 1 Introduction | 1 |
| 1.1 General | 1 |
| 1.2 Literature Review | 2 |
| 1.3 Organization of the Thesis | 3 |
| | |
| 2 Power Line Conditioners | 5 |
| 2.1 Power Quality: an Overview | 5 |
| 2.1.1 Causes for PQ deterioration | 5 |
| 2.1.2 Terms related to PQ | 6 |
| 2.2 Harmonics in Power Line | 7 |
| 2.2.1 Sources of Harmonics in Power Line | 7 |
| 2.2.2 Industrial Standards | 8 |
| 2.2.3 Effects of Distortion | 9 |
| 2.3 Power Line Conditioners as Solution to PQ Problems | 9 |
| 2.3.1 Active Filter Topologies | 10 |
| 2.3.2 AF Applications | 13 |
| | |
| 3 Current Source Based Line Conditioners | 14 |
| 3.1 Voltage Source and Current Source based Active Filters | 14 |
| 3.2 Different Topologies for CSAF | 14 |
| 3.2.1 3-Single phase & single 3-phase | 14 |
| 3.2.2 Modular and Single Inverter Approach | 15 |
| 3.3 Power Circuit for CSAPF | 16 |
| 3.3.1 DC Link Reactor | 16 |
| 3.3.2 The output passive filter | 17 |
| 3.3.3 Semiconductor devices and constraints | 18 |
| 3.3.4 Over-voltage Protection of CSI | 19 |
| 3.4 Current PWM | 19 |
| | |
| 4 Conventional Hysteresis Control for CSAPF | 21 |
| 4.1 Main circuit | 21 |
| 4.2 Derivation of reference signals | 22 |
| 4.3 Hysteresis Control | 24 |
| 4.4 Modeling and Simulation Results | 25 |

| | | |
|----------|---|-----------|
| 5 | Space Vector Modulated CSAPF | 34 |
| 5.1 | Space Vector Modulation Technique | 34 |
| 5.1.1 | Modulation of a Voltage-Source PWM Bridge | 34 |
| 5.1.2 | Modulation of a Current-Source PWM Bridge | 35 |
| 5.2 | SVM Implementation for CSAPF | 37 |
| 5.2.1 | Derivation of reference signals | 37 |
| 5.2.2 | Generation of Switching Functions | 38 |
| 5.2.3 | PWM Pattern Generation | 42 |
| 5.3 | Modeling and Simulation Results | 43 |
| | | |
| 6 | Artificial Neural Networks | 50 |
| 6.1 | Neuron Model | 51 |
| 6.2 | Perceptrons | 52 |
| 6.3 | Back propagation Networks | 52 |
| 6.4 | Counter propagation Neural Networks (CPNN) | 53 |
| | | |
| 7 | Ann Approach to SVM implementation for CSAPF | 54 |
| 7.1 | Proposed Network | 54 |
| 7.2 | Calculation Method | 56 |
| 7.3 | Modeling and Simulation Results | 59 |
| 7.4 | A Comparative Study | 68 |
| | | |
| 8 | Conclusion and Future Scope | 69 |
| | | |
| | <i>References</i> | <i>71</i> |

CHAPTER-1

INTRODUCTION

1.1 General

Solid state control of ac power using thyristors and other semiconductor switches is widely employed to feed controlled electric power to electrical loads, such as adjustable speed drives (ASD's), furnaces, computer power supplies, etc. Such controllers are also used in HV dc systems and renewable electrical power generation. These nonlinear devices inject harmonic currents in the AC system and increase overall reactive power demanded by the equivalent load. In order to keep power quality under limits proposed by standards, it is necessary to include some sort of compensation.

Passive filters have the demerits of fixed compensation, large size, and resonance. The increased severity of harmonic pollution in power networks has attracted the attention of power electronics and power system engineers to develop dynamic and adjustable solutions to the power quality problems. Such equipment, generally known as active power filters (APF's), are also called active power line conditioners (APLC's), instantaneous reactive power compensators (IRPC's), active power filters (APF's), and active power quality conditioners (APQC's). In recent years, many publications have also appeared on the harmonics, reactive power, load balancing, and neutral current compensation associated with linear and nonlinear loads.

With regard to their power circuit topology, active power filters can be categorized into two basic structures:

- 1) Voltage source active power filter (VSAPF)
- 2) Current source power active filter (CSAPF)

The CSAPF has a dc reactor with a dc current, whereas the VSAF has a capacitor on the dc side with a dc voltage. Although the voltage-source type is better with regard to loss and the filter capacity to eliminate the PWM carrier harmonics, the current source type is better with regard to reliability and protection. Further, considering the use of a superconducting magnet in the near future, the current-source type may be a practical solution, especially when the active filter is required to compensate not only the ordinary harmonics but also the sub and super harmonics related to the variation of the active power.

There are sinusoidal, hysteresis and space vector PWM controls as available techniques to control the current waveform of PWM converters. The hysteresis PWM control is simple, but its average switching frequency varies with load conditions so that switching patterns are uneven and random. The space vector modulation (SVM) technique, with some modifications, can be implemented for Current Source APF. The modified SVM technique is well matched with the requirement of instantaneous reactive power compensation.

The Artificial Neural Networks can be effective to improve the conventional SVM approach. The technique reduces software complexity, and computation time, and increases the accuracy of the positioning of the switching instants. The technique exhibits the following features: (a) possibility of higher switching frequencies, (b) higher band-width of the control loops, (c) reduced hardware and software, and (d) reduction of parasitic harmonics in all PWM waveforms.

1.2 Literature Review

The main issue of active filtering is to generate the harmonic and reactive part of the load current. The early works were dedicated with voltage source topologies. B. Singh, K. Al Haddad and A. Chandra, in their publications in 1997 [4] titled, "A New Control Approach to Three-phase Active Filter for Harmonics and Reactive Power Compensation" presents the hysteresis control for voltage source active power filters. This paper deals with a new control scheme for a parallel 3-phase active filter to eliminate harmonics and to compensate the reactive power of the non-linear loads. A modified hysteresis control for current source topology came in 2001 by D. Graovac, V. Kati, A. Rufer and J. Kne [6] titled, "Unified power quality conditioner based on Current Source Converter topology". In this paper a unified power quality conditioner based on current source converter topology was presented. It consists of two three-phase current-source converters of one of which is a current-source rectifier and another is a current-source inverter. Control structures, together with converter gating generation were presented. The space vector modulation technique for current source APF is first presented by E.H. Song and B.K. Kwon in their paper [7] "A Novel Digital Control for Active Power Filters". A SVM technique for the PWM converter is developed in order to generate desired current vectors of the APF for compensating both harmonic and reactive powers. In the paper [8], published in 2000, titled "A New Control Method for a Current-Source Active

Power Filter”, M. Salo and H. Tuusa presented the control technique for the space vector modulated CSAPF. The harmonic current compensation is realized using combined feed forward control of the load currents and closed-loop control of the supply currents. They referred the paper of 1993 by B.H. Kown and B. Min [9] titled “A Fully Software-Controlled PWM Rectifier with Current Link” for implementation of SVM technique for Current Source Converters. M. Routimo, M. Salo and H. Tuusa in there paper [10] titled “Comparison of Voltage-Source and Current-Source Shunt Active Power Filters” presents a comparative study of Voltage-Source and Current-Source Shunt Active Power Filters with hardware implementation. A. Bakhshai, J. Espinoza, G. Joos and H. Jin in there paper [12] published in 1996, titled “A Combined Artificial Neural Network and DSP approach to the implementation of Space Vector Modulation Techniques”, proposed a Counter Propagation Neural Network for implementation of SVM technique for rectifiers. This paper presents an alternative SVM implementation that is based on a neural network structure and its classification properties. The technique reduces hardware and software complexity, computation time, and increases the accuracy of the positioning of the switching instants.

1.3 Organization of the Thesis

The contents of this dissertation are organized in six chapters in the following manner. Chapter 1 introduces the power line conditioners and their uses for line compensation. It also mentions the several topologies and implementation techniques of power filters. Then, a review of the previous work in the area of the related field is addressed.

In Chapter 2, the power quality problems are discussed. It also includes the remedies of those problems by line conditioning techniques.

Chapter 3 deals with the current source based topologies of power filters. It also includes the overall structure and functioning of Current Source Active Power Filters (CSAPF).

Chapter 4 presents the hysteresis control techniques for CSAPF. A model is developed using MATLAB simulink. Simulation results are obtained for different loading conditions.

Chapter 5 presents a modified Space Vector Modulation (SVM) technique for CSAPF. The implementation is verified with a simulink model.

Chapter 6 introduces the Artificial Neural Networks (ANN).

In Chapter 7 an ANN approach is proposed for SVM implementation for CSAPF. A model is developed using MATLAB simulink. Simulation results are obtained for different loading conditions. Dynamic performance of the system is also studied.

In Chapter 8, Conclusion is drawn from the work done and presented. Future scope for improvements in the same field to improve the performance is presented to carry out in upcoming projects.

CHAPTER-2

POWER LINE CONDITIONERS

Power line conditioners or, more specifically, Active power filters are offering unprecedented ability to clean the network from harmonics. They eliminate harmonics in a controlled way and can compensate load unbalances and power factor at the same time. Present devices can eliminate up to the 50th harmonic, with a programmable filtering strategy and free choice of harmonics.

With the new semiconductor devices and topologies coming in the near future, active power filters will increase their ability to keep the power distribution systems clean and free of dangerous perturbations. However, at the same time, electronic equipment will become more and more sensitive to power quality disturbances. For these two reasons, active power filters have a growing challenge in keeping the system completely free of unwanted harmonics. Research and development will have to continue for this purpose. Before going to discussions with power line conditioners lets take an overview of problems related to power quality.

2.1 Power Quality: an overview

The term electric power quality broadly refers to maintaining a near sinusoidal power distribution bus voltage at rated magnitude and frequency. In addition, the energy supplied to a consumer must be uninterrupted from reliability point of view. Though power quality is mainly a distribution system problem power transmission system may also have impact on quality of power.

2.1.1 Causes for PQ deterioration

Causes for power quality deterioration can be classified in the two following categories:

1. natural causes
 - Fault or lightning sticks on line
 - Equipment failure
2. Man made causes
 - Transformer excitation, capacitor or feeder switching

- Power electronic loads as UPS, ASD, converters
- Arc furnaces, and induction heating systems
- Switching on and off of large loads

2.1.2 Terms related to PQ

Most of the more important international standards define power quality as the physical characteristics of the electrical supply provided under normal operating conditions that do not disrupt or disturb the customer's processes. Therefore, a power quality problem exists if any voltage, current or frequency deviation results in a failure or in a bad operation of customer's equipment. However, it is important to notice that the quality of power supply implies basically voltage quality and supply reliability. Voltage quality problems relate to any failure of equipment due to deviations of the line voltage from its nominal characteristics, and the supply reliability is characterized by its adequacy (ability to supply the load), security (ability to withstand sudden disturbances such as system faults) and availability (focusing especially on long interruptions). It is therefore important to list the terms that are used with power quality

- Transients
- Short duration voltage variation
- Long duration voltage variation
- Voltage imbalance
- Waveform distortion
- Voltage fluctuation
- Power frequency variations
- Poor load power factor
- Harmonic contents in loads
- DC offset in load voltage
- Supply voltage distortion
- Voltage sag/swell
- Voltage flicker

Power quality variations are classified as either disturbances or steady state variations. Disturbances are pertaining to abnormalities in the system voltages and or currents due to fault or some abnormal operations. Steady state variations refer to R.M.S. deviations from the nominal quantities or harmonics.

Power system harmonics, which is a specific power quality issue, is an area that is receiving a great deal of attention recently. This is primarily due to the fact that non-linear; arc loads are comprising a larger and larger portion of the total connected load for a typical industrial plant. If power factor correction capacitors are applied to a power system the results could be disastrous in some instances without due consideration to natural frequencies of the system and harmonic producing loads. If a resonance occurs there is a potential for capacitor has blowing or premature equipment failure, or transformer or motor overheating.

2.2 Harmonics in Power Line

Harmonics are a mathematical way of describing distortion to a voltage or current waveform, are a continuous, steady state phenomenon, and should not be confused with spikes surges or other forms of power system transients. Fourier theory tells us that any repetitive waveform can be expressed as the summation of a number of sinusoids of various frequencies. Harmonics, by definition, are components of a waveforms which are integer multiples of the fundamental frequency to address harmonic concerns prior to the addition of large non-linear loads by performing harmonic modeling analysis.

2.2.1 Sources of Harmonics in Power Line

- Transformer saturation
- Transformer inrush
- Transformer neutral connections
- MMF distribution in AC rotating machines
- Electric arc furnaces
- Fluorescent lighting
- Computer SMPS
- Battery chargers
- Impact of AC sources
- Static VAR compensators
- Adjustable Speed Drives(ASD's)
- DC Converters

- Inverters
- Television power supplies

2.2.2 Industrial Standards

The issue of increasing harmonic levels from power system engineering point of view is one of capacity. Generally the utility consumer electric supply is robust and tolerate nonlinear load to some extent. Voltage distortion in premises wiring is typically less than 5%. It probably could go higher than 5% without significant effect on the loads.

The problem for power system comes from the fact that with predominantly nonlinear loads the current distortion in the system is very high (>40% is unusual). The increased reactive current consumes the reserve capacity that is usually built into power system. The power system is likely to show problems before the load. Consider the added heating on a three phase motor in presence of 5% VTHD compared to the service transformer that is handling the related 60% ITHD, with high cost factor and neutral current. The transformer may need to be de-rated to less than 50% of capacity while the added motor loss is not noticed. In general high harmonic levels are more stressful on power system components than on loads.

New tougher standards limiting harmonic distortions in power systems are emerging internationally. Several difficulties appeared in applications of these standards:

1. Setting relevant limits for industrial equipment before this equipment is installed in the power system.
2. Establishing the share of financial responsibility between equipment manufacturer and user/consumer, and the electric power supplier after the equipment is installed.
3. Measuring compliances of individual equipment before installation and individual consumer at PCC after installation.

Harmonic standards are still evolving. To backup evolutionary process more technical work is needed in power system testing, analysis and simulation of harmonic propagation and effects.

2.2.3 Effects of Distortion

The voltage and current distortions in power system can hamper the system stability. There are other effects on both power system equipments and loads which are given below in a tabular form.

TABLE I
Effects of harmonic distortions on power system

| | Intermittent effects | Steady-state effects |
|---------------------------|---|---|
| Current distortion | <ul style="list-style-type: none"> * Improper operation of protection relays * Voltage distortion due to resonance | <ul style="list-style-type: none"> * Increased loss in series components in transmission, distribution and building wiring * Decreased accuracy in instruments (metering) * Voltage distortion due to ISC/IL |
| Voltage distortion | <ul style="list-style-type: none"> * Improper operation of protection relays * Disruption of harmonic sensitive loads | <ul style="list-style-type: none"> * Increased loss in capacitors, transformers and motors * Decreased accuracy in instruments (metering) |

2.3 Power Line Conditioners as Solution to PQ Problems

There are two approaches to the mitigation of power quality problems. The first approach is called load conditioning, which ensures that the equipment is made less sensitive to power disturbances, allowing the operation even under significant voltage distortion. The other solution is to install line-conditioning systems that suppress or counteract the power system disturbances. Passive filters have been most commonly used to limit the flow of harmonic currents in distribution systems. They are usually custom designed for the application. However, the problems with passive filters are:

1. The source impedance which is not accurately known and varies with the system configuration, strongly influences the filtering characteristics of the shunt passive filters
2. The shunt passive filters acts as a sink to the harmonic current flowing from the source. In the worst case, the shunt passive filter may fall in series resonance with the source impedance.
3. At a specific frequency, an anti-resonance or parallel resonance may occur between the source impedance and the shunt passive filter, which is called harmonic amplification.
4. As both the harmonics and the fundamental current components flow into the filter, the capacity of the filter must be ratted by taking into account both the currents.
5. Increase in harmonic current component can overload the filter.
6. Also, if a good level of correction is targeted; one needs as many filters as the no. of harmonic to be eliminated.

Among the different new technical options available to improve power quality, active power filters have proved to be an important and flexible alternative to compensate for current and voltage disturbances in power distribution systems. The idea of active filters is relatively old, but their practical development was made possible with the new improvements in power electronics and microcomputer control strategies as well as with cost reduction in electronic components. Active power filters are becoming a viable alternative to passive filters and are gaining market share speedily as their cost becomes competitive with the passive variety.

2.3.1 Active Filter Topologies

Depending on the particular application or electrical problem to be solved, active power filters can be implemented as shunt type, series type, or a combination of shunt and series active filters (shunt-series type). These filters can also be combined with passive filters to create hybrid power filters.

(A) Shunt Active Filters

Shunt active power filters compensate load current harmonics by injecting equal but opposite harmonic compensating current. In this case the shunt active power filter operates as a current source injecting the harmonic components generated by the

load but phase-shifted by 180°. Fig. 1 shows how the active filter works to compensate the load harmonic currents.

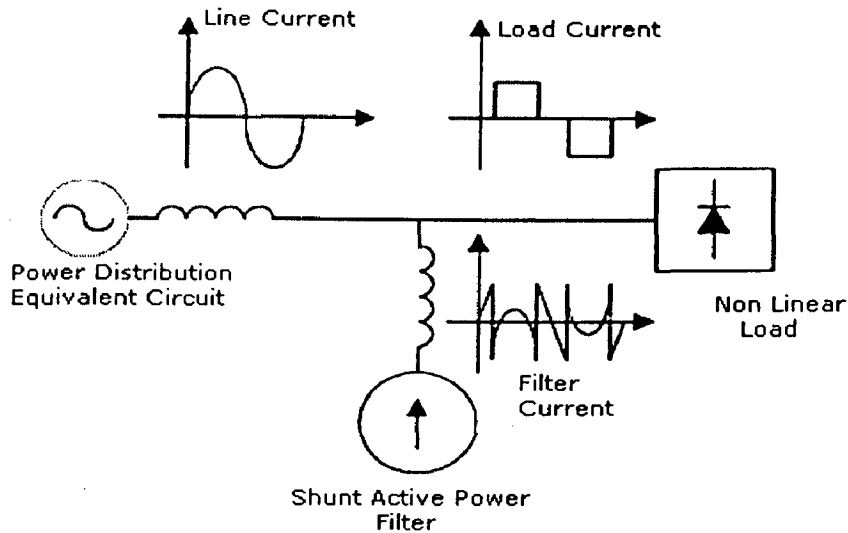


Fig. 1: Shunt Active Power Filter

Mainly two types of converters are used for the developments of active power filters:

1. A Voltage source PWM converter
2. A current source PWM converter

A voltage source PWM converter based active power filter has a self supporting DC voltage with a DC capacitor as shown. Its use is reported widely due to its high efficiency, light weight, low cost and expendability to multilevel and multi step versions.

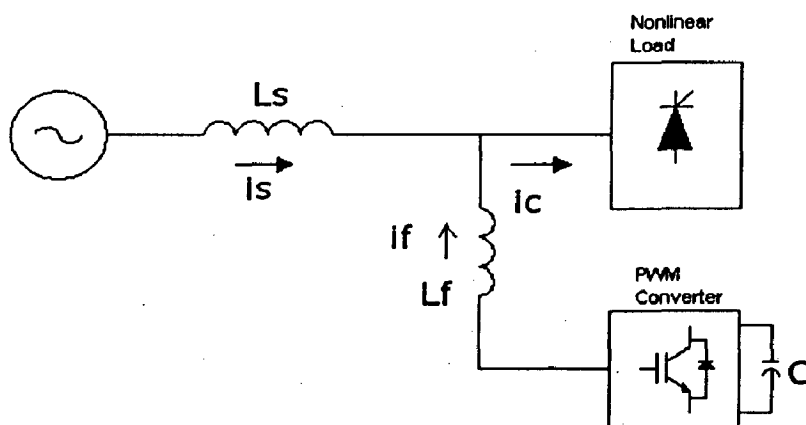


Fig. 2: Voltage Source Shunt Active Power Filter

Fig.3 shows the current source PWM converter based APF. It behaves as a non-sinusoidal current source to meet the harmonic current requirements of the non-linear load. Although, they are considered sufficiently reliable but requirement of a DC Link reactor is the main limitation of this type of converter.

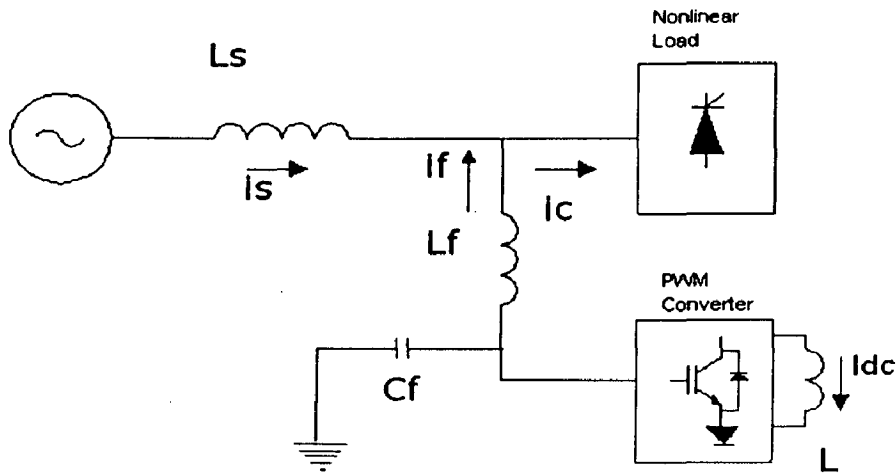


Fig. 3: Current Source Shunt Active Power Filter

(B) Series Active Filter

The series active filter injects a voltage component in series with the supply voltage and therefore can be regarded as a controlled voltage source, compensating voltage sags and swells on the load side. In many cases, series active filters work as hybrid topologies with passive LC filters. If passive LC filters are connected in parallel to the load, the series active power filter operates as a harmonic isolator, forcing the load current harmonics to circulate mainly through the passive filter rather than the power distribution system. However, the apparent power rating of the series active power filter may increase in case of voltage compensation.

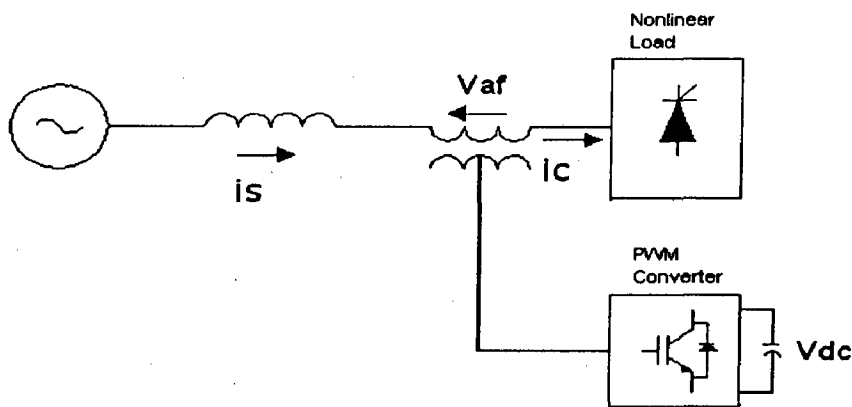


Fig. 4: Series Active Power Filter

Fig.4 shows the configuration of a Series Active Power Filter. It is connected before the load in series with the mains using the matching transformer. It is mainly used to eliminate voltage harmonics, to reduce the negative sequence voltage and regulate the voltage on the three phase system. It is mainly installed by the utilities to compensate voltage harmonics and damping harmonic propagation.

(C) Series Shunt Active Filters

As the name suggests, the series-shunt active filter is a combination of the series active filter and the shunt active filter. The shunt active filter is located at the load side and can be used to compensate for the load harmonics. On the other hand, the series portion is at the source side and can act as a harmonic blocking filter. This topology has been called the Unified Power Quality Conditioner (UPQC). The series portion compensates for supply voltage harmonics and voltage unbalances, acts as a harmonic blocking filter, and damps power system oscillations.

The shunt portion compensates load current harmonics, reactive power, and load current unbalances. In addition, it regulates the dc link capacitor voltage. The power supplied or absorbed by the shunt portion is the power required by the series compensator and the

2.3.2 AF Applications

Active power filters are typically based on GTOs or IGBTs, voltage source PWM converters, connected to medium- and low-voltage distribution systems in shunt, series, or both topologies at the same time. In comparison to conventional passive LC filters, active power filters offer very fast control response and more flexibility in defining the required control tasks for particular applications. The selection of equipment for improvement of power quality depends on the source of the problem. If the objective is to reduce the network perturbations due to distorted load currents, the shunt connection is more appropriate. However, if the problem is to protect the consumer from supply-voltage disturbances, the series-connected power conditioner is most preferable. The combination of the two topologies gives a solution for both problems simultaneously.

CHAPTER-3

CURRENT SOURCE BASED LINE CONDITIONER

A current source inverter used as an active filter produces a non-sinusoidal current that compensates for the harmonic current drawn by a nonlinear load. The inverter switching frequency is nearly one order of magnitude higher than the highest frequency component to be compensated. A dc current source is realized with the inductor L_{dc} across the terminals of the CSI. The inductance value is primarily a function of the system volt-ampere rating and the range of harmonic levels of the load. By summing the maximum possible energy required to correct the 5th, 7th, 11th, and 13th harmonic components, the energy storage requirement for the inductor can be estimated.

3.1 Voltage Source and Current Source based Active Filters

Both Voltage Source and Current Source based Active Filters achieve the main target of the active filter and hence improve the power quality of the distribution system.

The major advantage of the VSAF structure is in its capacitive energy storage element which is more efficient, smaller and costs less than inductive one used in CSAF. Nevertheless, this advantage may become in favor of CSAF in near future when superconductor coils are practically used in higher temperatures.

A proper sizing of the output passive filter, through which the active filter is connected to the AC mains, must take into account the inverter switching frequency. The objectives claimed to this filter may be better satisfied with CSAF than VSAF.

3.2 Different Topologies for CSAF

3.2.1 3-Single phase & single 3-phase

Single phase active power filter is based on harmonic current injection into power network. It requires a current fed inverter and a DC current source with constant magnitude. However extending this scheme to poly phase system requires one independent single phase unit for each phase. Each single phase unit requires four (4) transistors thus total twelve (12) transistors are required for three-phase case as shown in Fig. 5.

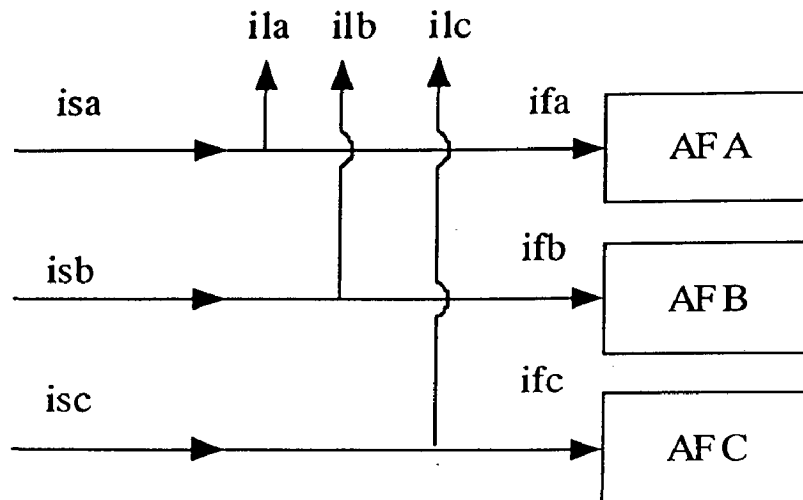


Fig. 5: 3-Single phase filter topology

The proposed three phase active power filter circuit shown in Fig. 6 provides harmonic cancellation of three phases in a single unit. Compared to previous scheme, the required power switches reduces from 12 to 6 and number of inductors from 3 to just 1. Further total installed VA capacity is reduced up to 50% whilst maintaining optimum performance.

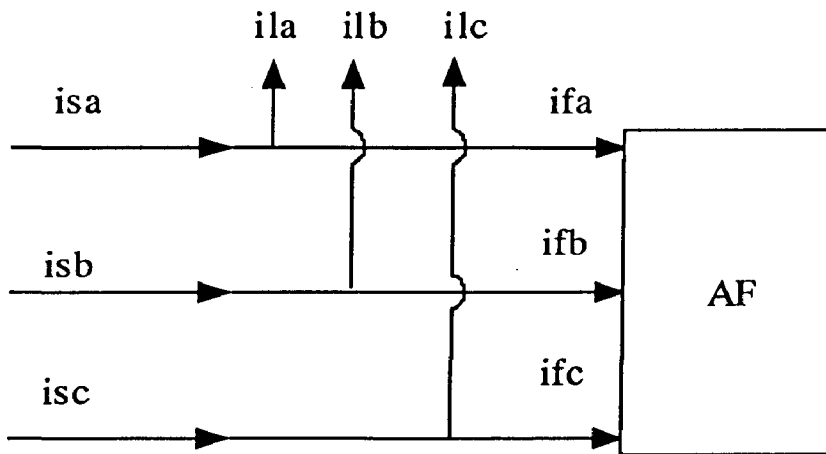


Fig. 6: Single 3-phase filter topology

3.2.2 Modular and Single Inverter Approach

Modular approach uses an inverter module for each harmonic to be eliminated from power line. Sinusoidal PWM technique can be employed for the inverter modules.

Since each inverter is independently connected to the AC system, selected harmonic elimination based on the dominant harmonic component is possible. This will result in

great flexibility and enhancement of the overall performance of the proposed active filter.

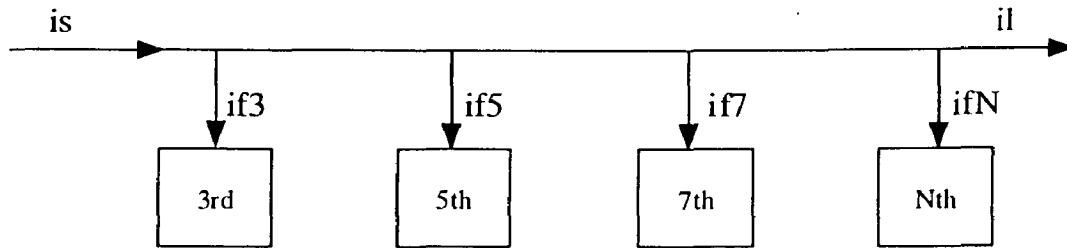


Fig. 7: Modular Approach of Power filters

The installation cost of the modular scheme will be higher than that of the 1-inverter approach. The single inverter approach uses only one inverter. So its configuration is simpler and it is better in regard to robustness. It is economic as well. But its control strategy is a bit complicated.

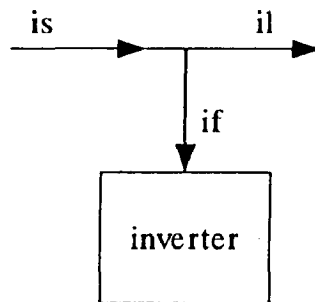


Fig. 8: Single Converter Approach of Power filters

Out of all these schemes the most general and most used scheme is Single three phase (single converter) one for economy, robustness and optimum VA capacity.

3.3 Power Circuit for CSAPF

The power circuit design of the CSAPF, involves selecting the parameters of the DC source and the elements of the AC output passive filter as well as the choice of the proper semiconductor devices for its structure.

3.3.1 DC Link Reactor

The selection of the DC current I_{dc} made in order to permit the active filter to be capable to follow its reference. The reactor in CSAF is designed in order to provide a DC current with acceptable ripples. The DC current, I_{dc} must be higher than the peak value of the harmonic current to be generated by the active filter. The inductance, L_{dc} is fixed by an allowable current ripple during each operation cycle.

For smoothing DC current and thus to improve the performance of the active filter, a large reactor should be used which increases the active filter's cost. In the case of high power applications, superconductor coils are the most reliable energy storage elements. Further, these elements have a large inductance resulting in dc current ripple elimination.

3.3.2 The output passive filter

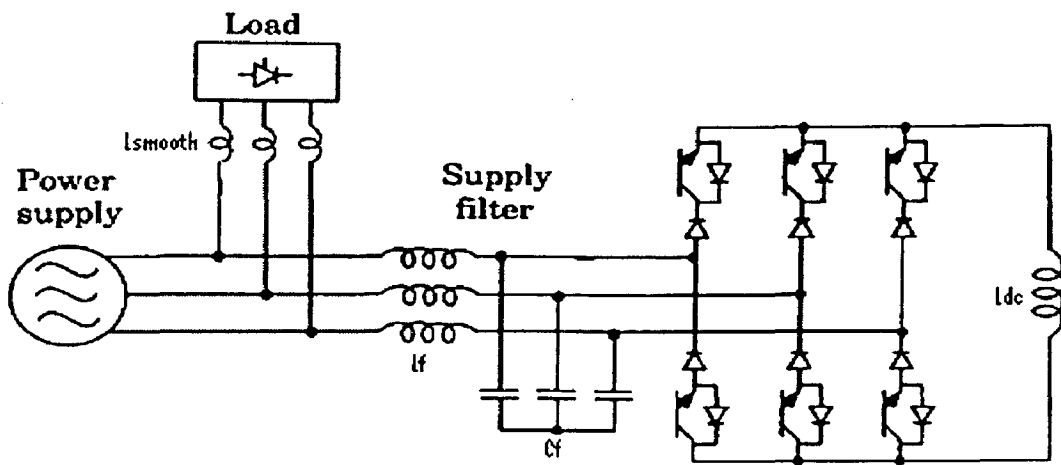
An active filter must be connected to the AC mains through a de coupling passive filter. The design of this filter should consider two points:

- Providing a sufficient attenuation of the high switching ripples caused by the inverter.
- Preserving high performance for the active filter.

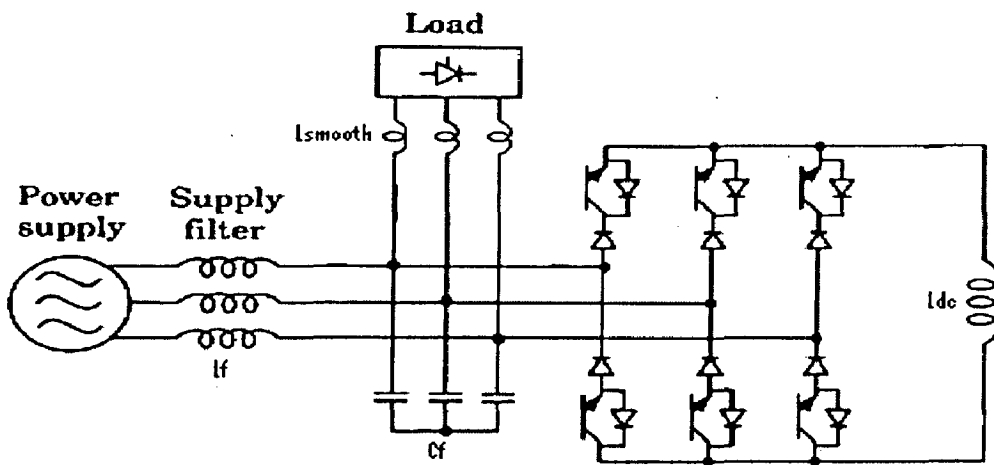
The optimized output filter, through which the CSAF is connected to the AC mains, is a second order low-pass filter realized by means of a capacitor Cf, and inductance Lf, as shown in Fig. 9. This filter offers a good compromise between a sufficient band-pass and a proper attenuation of switching harmonics. This can be accomplished by an accurate selection of the resonance frequency.

$$f_0 = \frac{1}{2\pi\sqrt{L_f * C_f}}$$

which must be larger than the highest harmonic frequency to be compensated and at the same time much lower than the inverter switching frequency. At a given resonance frequency, since the capacitor Cf protects the switching devices against the over voltage caused by the high current gradient in the inductance Lf, increasing Lf will result in decreasing Cf and consequently reduces the semiconductor protection. On the other hand, Lf must be chosen higher than the internal inductance of the AC mains. Thus, a compromise has to be made in order to obtain the optimum filter design. There are two topologies available for connecting the LC filter across the supply and the inverter. Fig. 9(a) shows the most common main circuit structure of the shunt-type current source active power filter where CSAF is connected in parallel with the load. The control system is usually realized by using the closed-loop control of the source current and the feed forward control of the load current.



(a)



(b)

Fig. 9: Arrangements of LC filter, (a) power filter is connected in parallel with the load, (b) the load is connected in parallel with the supply filter and the rectifier bridge.

In the main circuit structure shown in Fig. 9(b), the load is connected in parallel with the supply filter and the rectifier bridge. The control system realization is based on the measurement of the supply current resulting in modest filtering performance.

3.3.3 Semiconductor devices and constraints

In CSAF structure as illustrated in Fig. 9 the current is unidirectional and limited by the DC current source while the voltage is bipolar and its peak value corresponds to that of line voltage. So the suitable semiconductor device, in this case, may be a GTO with reverse voltage blocking Capability or an IGBT with series

connected diode and must be protected against over voltage. Actually IGBT transistor has lower losses and can operate at higher switching Frequencies than GTO thyristor.

3.3.4 Over-voltage Protection of CSI

The problems of protecting CSI are dual to the problem occurring with VSI. With VSI the main problem is protection against over-currents. Dual to that, the most difficult task is the protection of the CSI against over-voltages. The protection of CSI from over-currents is quite simple, because the rate of current change is limited to a very small value by the DC link choke. It can easily be done by an appropriate control of DC link current.

Causes

Over-voltages are primarily caused by the following effects:

- Error in switching patterns for the semiconductors
- Small systematic over-voltages from the commutation inductances between input filter and inverter
- Over-voltages from the mains or from the load
- Self excitation with an asynchronous machine as load

Remedies

Three kinds of over-voltage protections for a CSI are imaginable:

1. In a VSI a semiconductor which conducts to big a current can be protected by turn-off. Dual to that in a CSI the protection of an element which is stressed by to high a voltage can be done by turning on the element.
2. Every semiconductor can be equipped with an over-voltage limiter (VDR, MOV etc.).
3. A whole group of semiconductors can be protected by a single over-voltage limiter.

3.4 Current PWM

The carrier-modulated sine PWM and programmed PWM techniques are usually used for the inverter design. But sine PWM technique can not be implemented for a CSI based PLC as the later must satisfy the following requirements:

1) CSI must generate arbitrarily waveform currents that equal to compensation current with a minimal time delay.

2) One of the three upper arm switches and one of the three lower arm switches must be ON state simultaneously.

Hence programmed PWM techniques are used where switching patterns are computed by some optimization algorithm. The low order harmonics can be completely eliminated from the line by the computed switching pattern and the high order harmonics can be suppressed by a passive filter. Thus, a high quality sinusoidal output waveform for the line current can be produced.

CHAPTER-4

CONVENTIONAL HYSTERESIS CONTROL FOR CSAPF

Among the various PWM techniques, the hysteresis band current control is used very often because of its simplicity of implementation. Also, besides fast response current loop, the method does not need any knowledge of load parameters. The basic implementation of hysteresis current control is based on deriving the switching signals from the comparison of the current error with a fixed tolerance band. This control is based on the comparison of the actual phase current with the tolerance band around the reference current associated with that phase. However, the current control with a fixed hysteresis band has the disadvantage that the PWM frequency varies within a band because peak-to-peak current ripple is required to be controlled at all points of the fundamental frequency wave. Moreover, this type of band control is negatively affected by the phase current interactions which is typical in three-phase systems. This is mainly due to the interference between the commutations of the three phases, since each phase current not only depends on the corresponding phase voltage but is also affected by the voltage of the other two phases. Depending on load conditions switching frequency may vary during the fundamental period, resulting in irregular inverter operation. In this chapter, the current control of PWM-CSAPF has been implemented with instantaneous reactive and harmonic power compensation.

The control strategy has been implemented in two parts:

1. Derivation of reference signals
2. Generation of PWM patterns with Hysteresis Control

4.1 Main circuit

Fig 10 shows a system configuration of the current source active power filter, installed for compensating both the reactive power and harmonic current generated by the three phase full wave diode bridge rectifier. The active power filter system consists of a current source PWM converter. The LC filters are used to suppress the switching ripples generated by the APF.

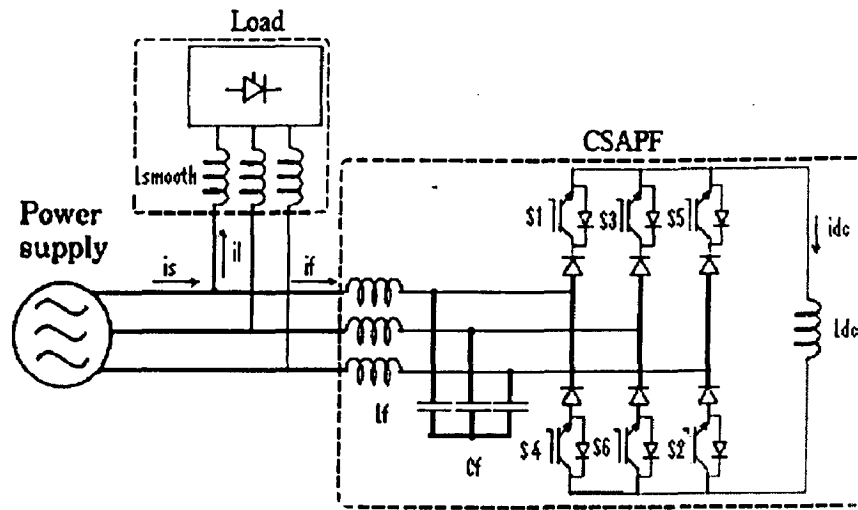


Fig 10: Main Circuit of CSAPF.

4.2 Derivation of reference signals

The APF is to compensate the reactive and harmonic components of the load current so that the source current may only consists of sinusoidal and in phase components with the source voltage. The source voltage v and the load current i_l are measured and transformed into x-y orthogonal coordinate according to the following expressions [7]

$$\begin{bmatrix} v_x \\ v_y \end{bmatrix} = \begin{bmatrix} 1 & -1/2 & -1/2 \\ 0 & \sqrt{3}/2 & -\sqrt{3}/2 \end{bmatrix} \begin{bmatrix} v_a \\ v_b \\ v_c \end{bmatrix} \dots \dots \dots 4.1$$

$$\begin{bmatrix} i_{l_x} \\ i_{l_y} \end{bmatrix} = \begin{bmatrix} 1 & -1/2 & -1/2 \\ 0 & \sqrt{3}/2 & -\sqrt{3}/2 \end{bmatrix} \begin{bmatrix} i_{l_a} \\ i_{l_b} \\ i_{l_c} \end{bmatrix} \dots \dots \dots 4.2$$

After coordinate transformation the vectors are invariant. It is possible to drive directly the compensating currents on x-y coordinate without the inverse transform. Moreover, considering the balanced three phase three wire system, these transformations are simplified as

$$\begin{aligned} v_x &= 3/2v_a \\ v_y &= \sqrt{3}v_a + \sqrt{3}v_b \dots \dots \dots 4.3 \end{aligned}$$

And

$$\begin{aligned} i_{l_x} &= 3/2i_{l_a} \\ i_{l_y} &= \sqrt{3}i_{l_a} + \sqrt{3}i_{l_b} \dots \dots \dots 4.4 \end{aligned}$$

Assuming the effects by LC filters are negligible, the instantaneous active power pl and instantaneous reactive power ql flowing into the load side are expressed as

$$\begin{bmatrix} pl \\ ql \end{bmatrix} = \begin{bmatrix} v_x & v_y \\ -v_y & v_x \end{bmatrix} \begin{bmatrix} il_x \\ il_y \end{bmatrix} \dots\dots\dots 4.5$$

The instantaneous powers pl and ql can be divided into two components

$$\begin{aligned} pl &= pl_{dc} + pl_{ac} \\ ql &= ql_{dc} + ql_{ac} \end{aligned} \dots\dots\dots 4.6$$

The DC components pl_{dc} and ql_{dc} correspond to the fundamental active and reactive power, respectively, and the AC components pl_{ac} and ql_{ac} corresponds to the harmonics of load current.

To compute Harmonic free unity power-factor, 3-phase currents, compensating powers p_c and q_c are selected as

$$\begin{aligned} p_c &= pl_{dc} + p_{loss} \\ q_c &= 0 \end{aligned} \dots\dots\dots 4.7$$

Where p_{loss} is the instantaneous active power corresponding to the switching loss and the resistive loss of the active power filter.

The x-y components of the fundamental current is obtained as follows

$$\begin{bmatrix} i_{1x} \\ i_{1y} \end{bmatrix} = \begin{bmatrix} v_x & v_y \\ -v_y & v_x \end{bmatrix}^{-1} \begin{bmatrix} p_c \\ q_c \end{bmatrix} \dots\dots\dots 4.8$$

The a-b-c components of the fundamental reference current is obtained as follows

$$\begin{bmatrix} i_{sa}^* \\ i_{sb}^* \\ i_{sc}^* \end{bmatrix} = \begin{bmatrix} 2/3 & 0 \\ -1/3 & 1/\sqrt{3} \\ -1/3 & -1/\sqrt{3} \end{bmatrix} \begin{bmatrix} i_{1x} \\ i_{1y} \end{bmatrix} \dots\dots\dots 4.9$$

4.3 Hysteresis Control

Harmonic free unity power-factor, 3-phase source currents are estimated according to the proceeding section. The reference current to the Hysteresis Based Current Controller is the difference between the actual source current and the estimated current [4].

$$\begin{aligned}
 i_{ea} &= i_{sa}^* - i_{sa} \\
 i_{eb} &= i_{sb}^* - i_{sb} \\
 i_{ec} &= i_{sc}^* - i_{sc}
 \end{aligned}
 \dots\dots\dots 4.10$$

The current controller decides the switching pattern of the AF devices. The switching logic is formulated as follows:

- If $i_{sa} > (i_{sa}^* + hb)$, the upper switch is OFF and lower switch is ON for leg A of the converter ($SB_A = 0$).
- If $i_{sa} < (i_{sa}^* - hb)$, the upper switch is ON and lower switch is OFF for leg A of the converter ($SB_A = 1$).

The bi-level switching functions SB_B and SB_C for phases B and C are determined similarly, using the corresponding reference and measured currents and the hysteresis band hb.

Current reference signals, as derived in preceding section, are compared to actual source current. Their difference (current error) is fed to hysteresis comparators forming the inverter bi-level switching signals SB. Output of the hysteresis controller yields bi-level switching signals for converter legs A, B and C, necessary for the converter control. Formation of the final transistor switching signals is based on the following procedure: from the bi-level signal ($SB_i, i=A,B,C$), a tri-level leg switching function signal ($ST_i, i=A,B,C$), necessary for proper operation of the converter, is derived [6]:

$$\begin{aligned}
 ST_A &= SB_A - SB_B \\
 ST_B &= SB_B - SB_C \\
 ST_C &= SB_C - SB_A
 \end{aligned}
 \dots\dots\dots 4.11$$

Then the bi-level switching functions of the transistors are:

$$\begin{aligned}
ST_1 &= \begin{cases} 1, ST_A > 0 \\ 0, otherwise \end{cases} & ST_4 &= \begin{cases} 1, ST_A < 0 \\ 0, otherwise \end{cases} \\
ST_3 &= \begin{cases} 1, ST_B > 0 \\ 0, otherwise \end{cases} & ST_6 &= \begin{cases} 1, ST_B < 0 \\ 0, otherwise \end{cases} \dots \dots 4.12 \\
ST_5 &= \begin{cases} 1, ST_C > 0 \\ 0, otherwise \end{cases} & ST_2 &= \begin{cases} 1, ST_C < 0 \\ 0, otherwise \end{cases}
\end{aligned}$$

For the inductive type loads, it is necessary to ensure the existence of the DC current path. If the inverter mode of operation is necessary, the alternative current path for the DC current must be obtained within the converter. Since only two of the switches are conducting at the same time (one in the upper and one in the lower part of the bridge), the gating signals can be derived from the bi-level transistor switching functions (ST_i , $i=1,\dots,6$) in the following manner:

$$\begin{aligned}
SW_1 &= ST_1 \vee (\overline{ST_1} \wedge \overline{ST_3} \wedge \overline{ST_5} \wedge ST_4) \\
SW_3 &= ST_3 \vee (\overline{ST_1} \wedge \overline{ST_3} \wedge \overline{ST_5} \wedge ST_6) \\
SW_5 &= ST_5 \vee (\overline{ST_1} \wedge \overline{ST_3} \wedge \overline{ST_5} \wedge ST_2) \\
SW_4 &= ST_4 \vee (\overline{ST_4} \wedge \overline{ST_6} \wedge \overline{ST_2} \wedge ST_1) \dots \dots \dots 4.13 \\
SW_6 &= ST_6 \vee (\overline{ST_4} \wedge \overline{ST_6} \wedge \overline{ST_2} \wedge ST_3) \\
SW_2 &= ST_2 \vee (\overline{ST_4} \wedge \overline{ST_6} \wedge \overline{ST_2} \wedge ST_5)
\end{aligned}$$

This means that the switch SW_i should be gated either when its tri-level function is active or when the complementary transistor is conductive, but none of the switches in the same part of the bridge (upper or lower) have active tri-level function.

4.4 Modeling and Simulation Results

A model is developed with the above equations in MATLAB simulink as shown in Fig 11 and 12. The parameters used for simulation are shown in Table II. However, 15 times the value given in the table is used for the supply filter resistance R_f , in order to model the increase of the resistance due to the skin effect at the filter resonance frequency. The hysteresis band is of 0.3A. As a harmonic source a three phase diode rectifier with RL-load ($R = 64 \text{ ohm}$, $L = 10 \text{ mH}$) is used. Also, the filter inductor of 2.0 mH is used in front

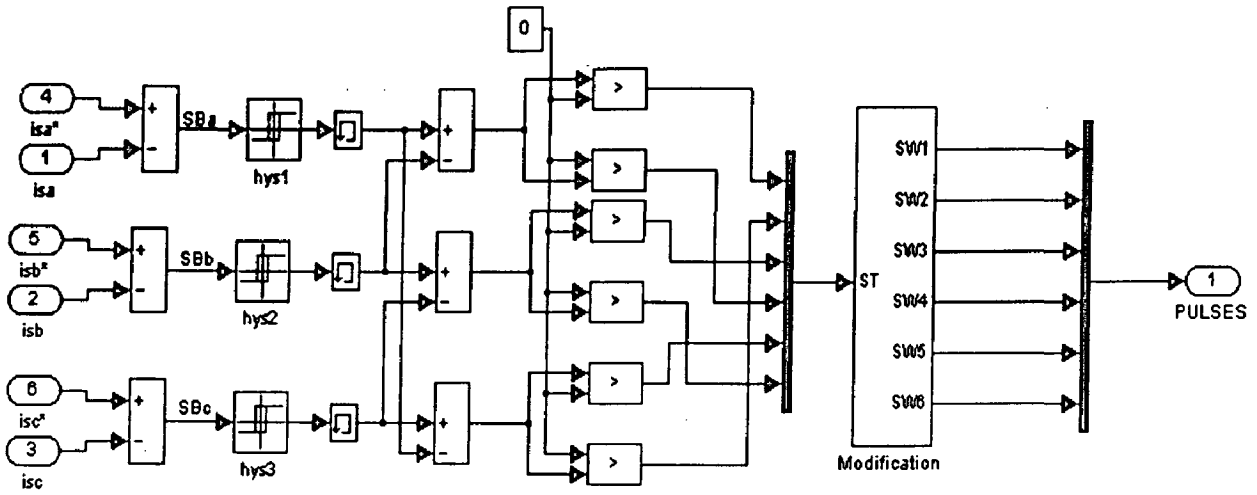


Fig. 12: Simulink Model for the Subsystem for the Hysteresis controller

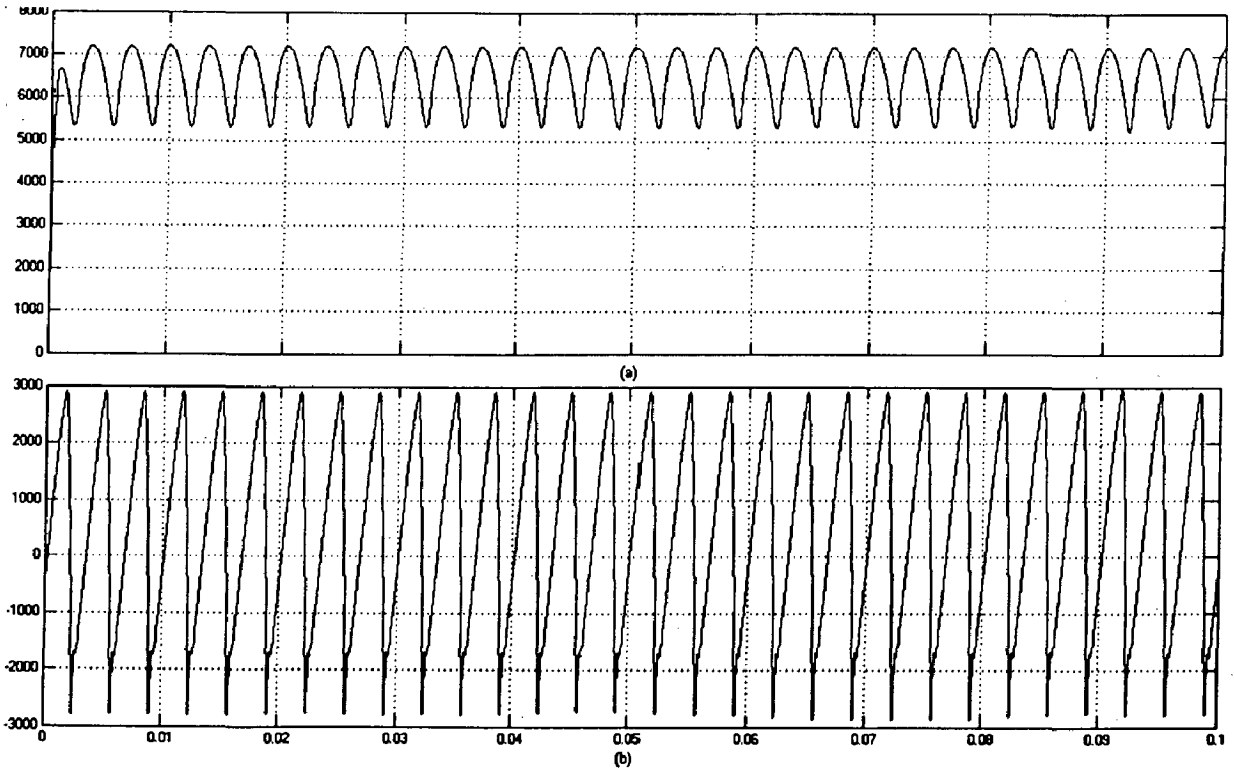


Fig. 13: Instantaneous power drawn from source by the diode bridge RL load
 (a) Instantaneous active power (W), (b) Instantaneous reactive power (VAR)

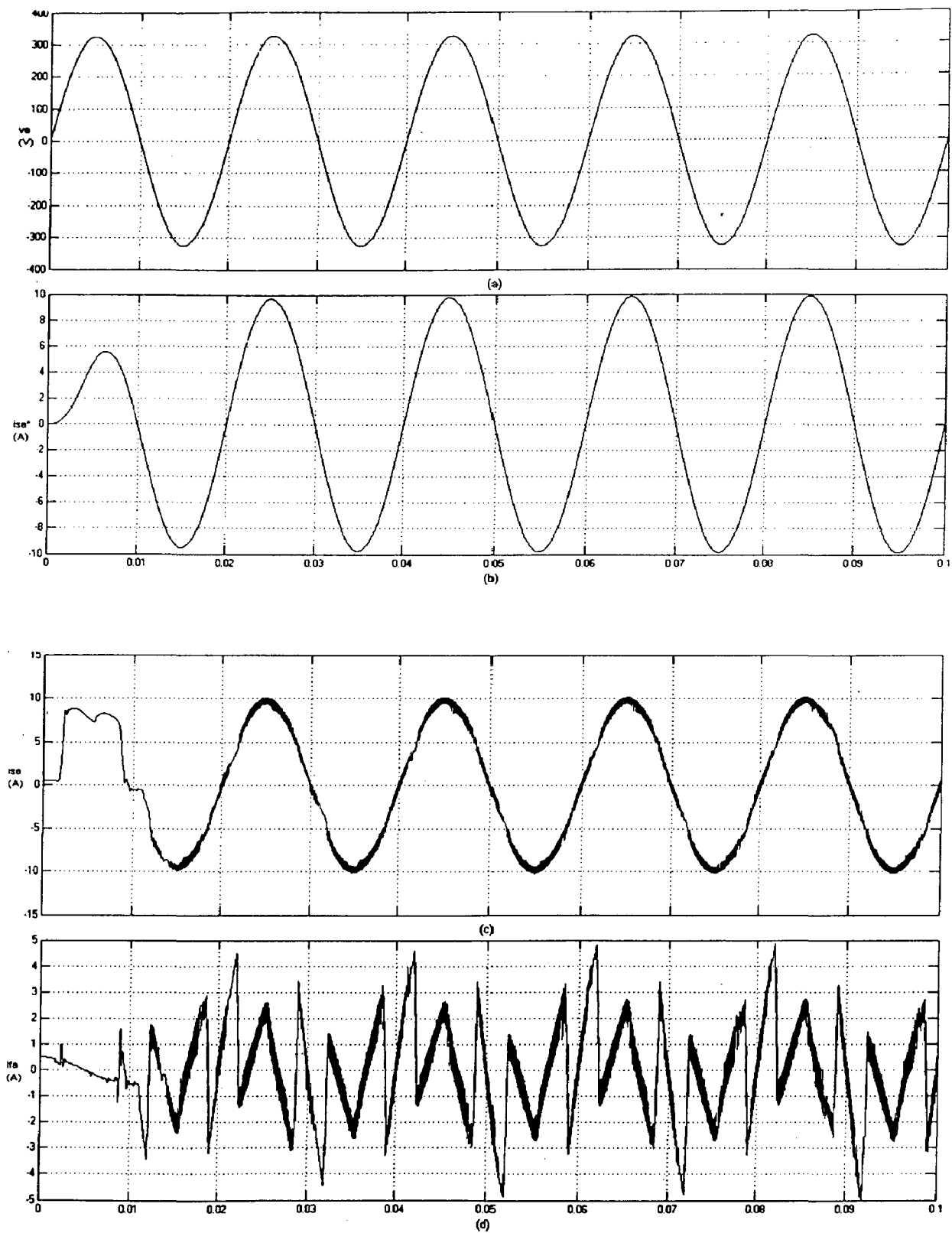


Fig.14: (a) Supply Voltage (V), (b) Reference Source Current (A),
(c) Source Current (A), (d) Filter Current (A) for RL Load

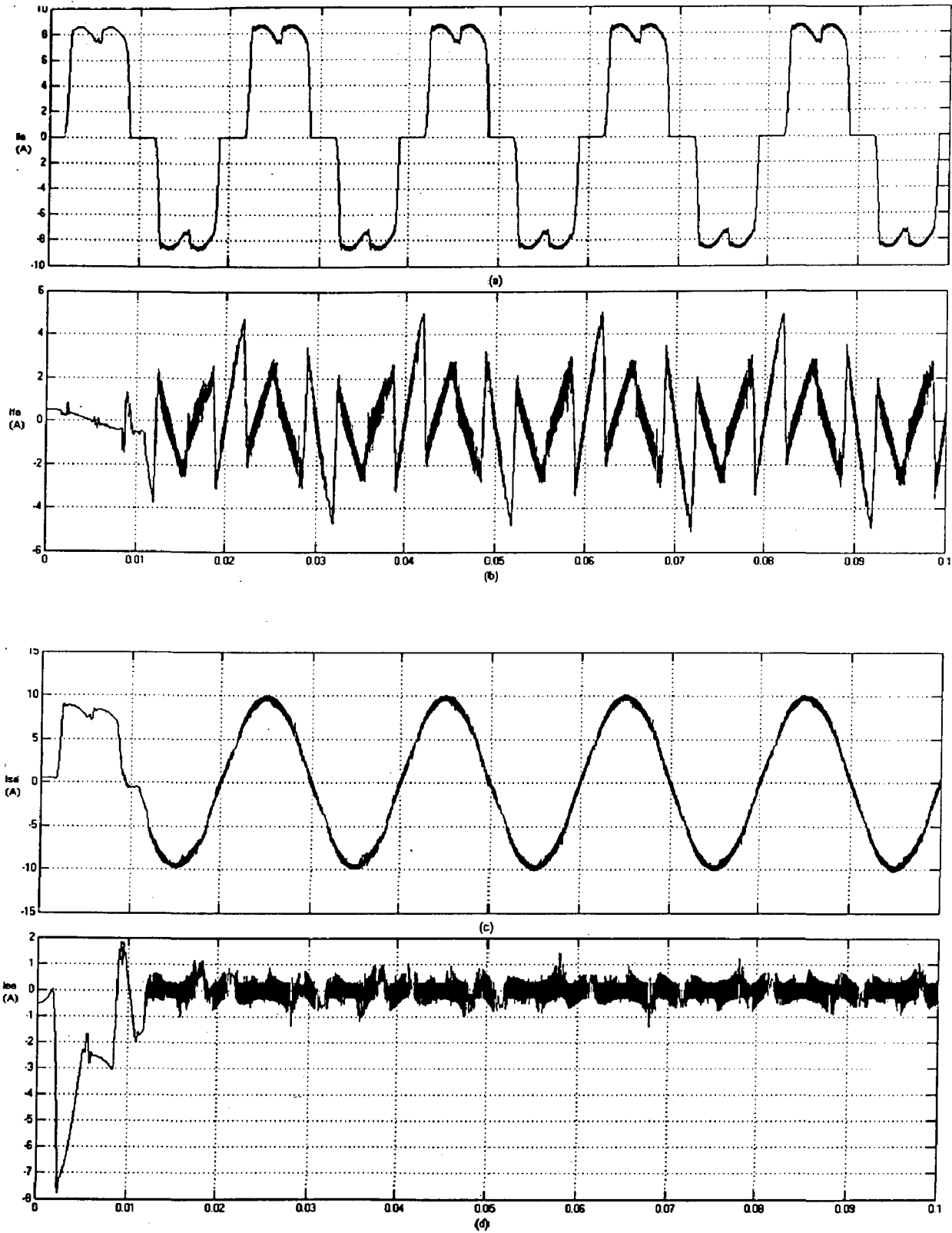
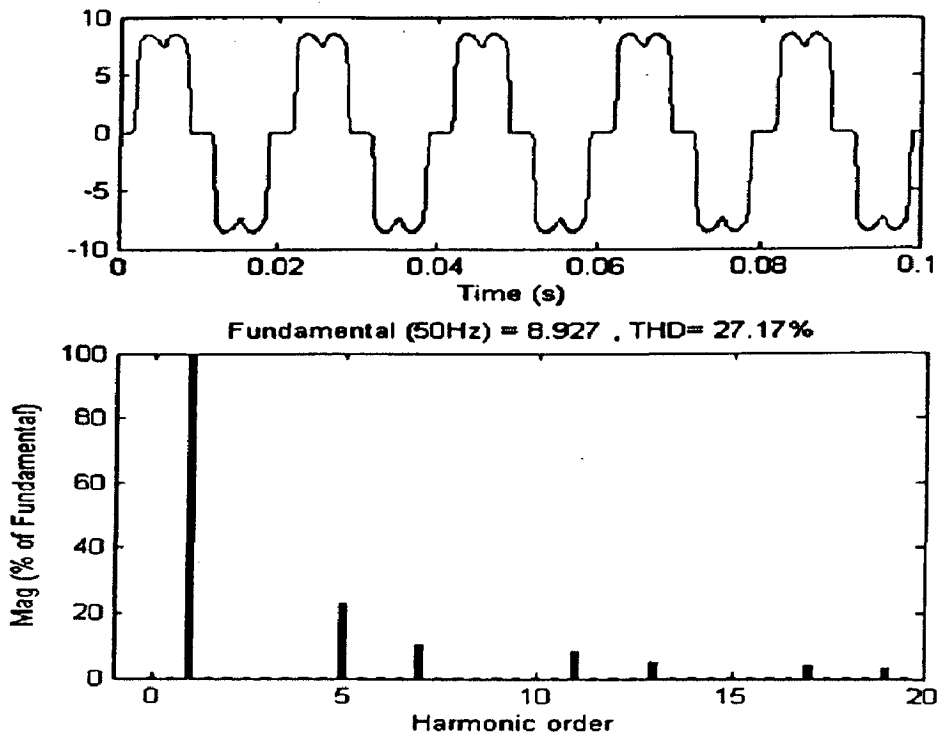
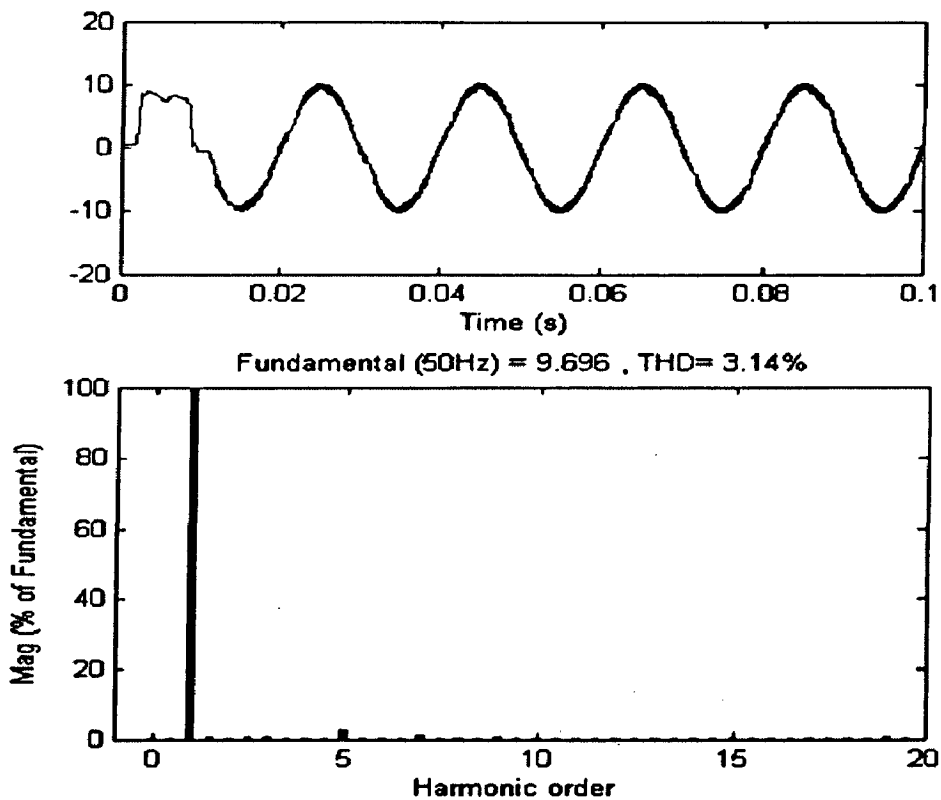


Fig. 15: (a) Load Current (A), (b) Filter Current (A), (c) Source Current (A)
 (d) Error Current (A) for RL Load



(a)



(b)

Fig. 16: FFT Analysis, (a) Load Current, (b) Source Current, for RL Load

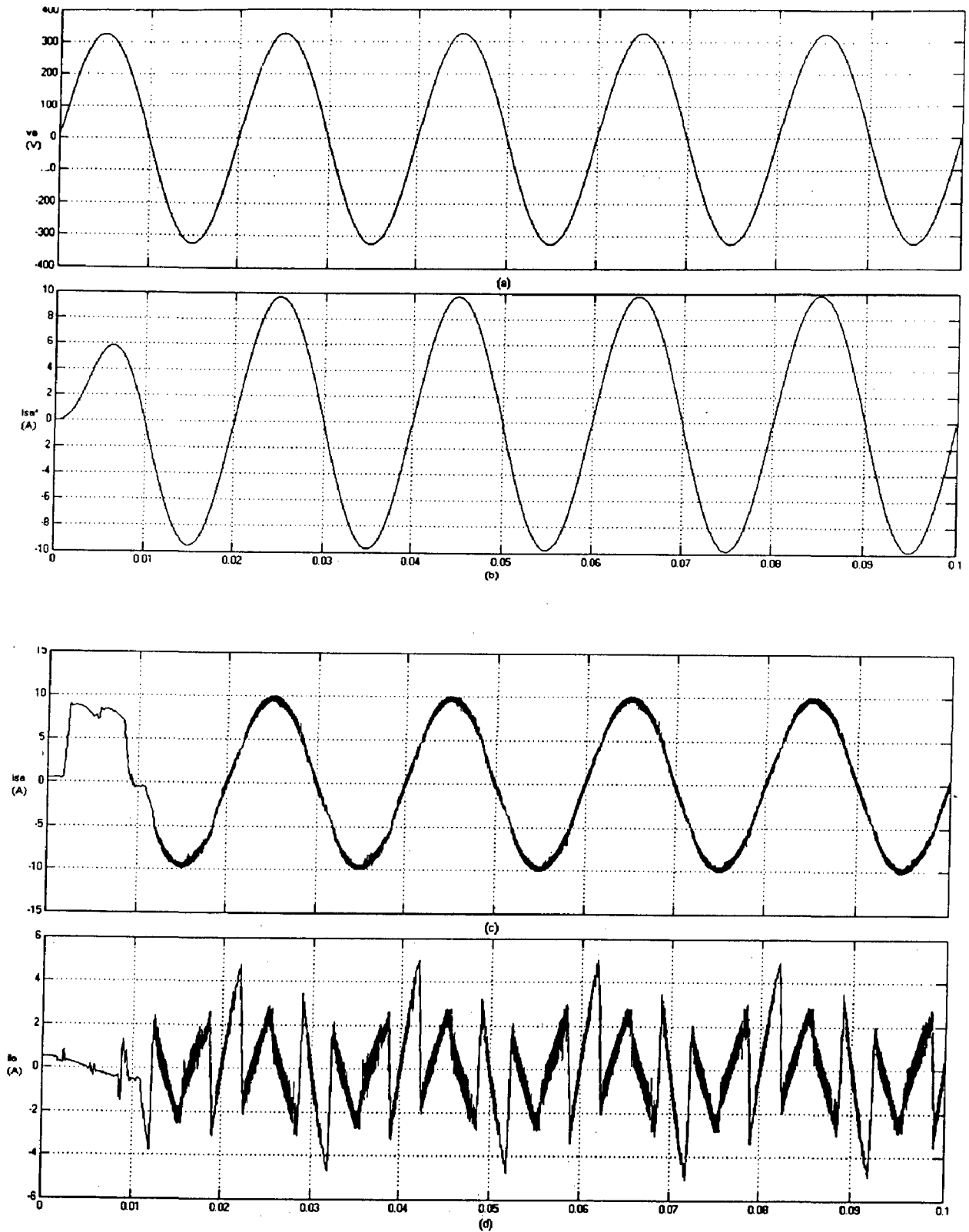


Fig.17: (a) Supply Voltage (V), (b) Reference Source Current (A),
(c) Source Current (A), (d) Filter Current (A) for RC Load

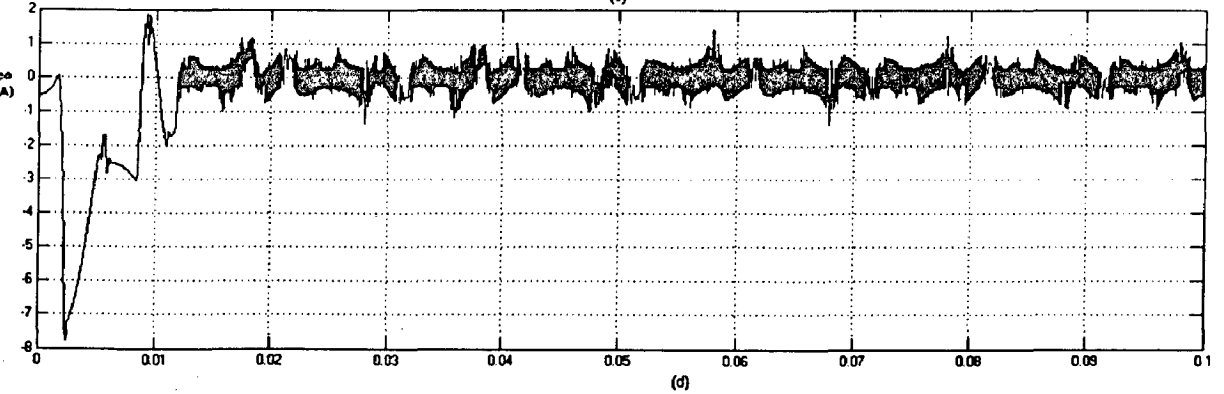
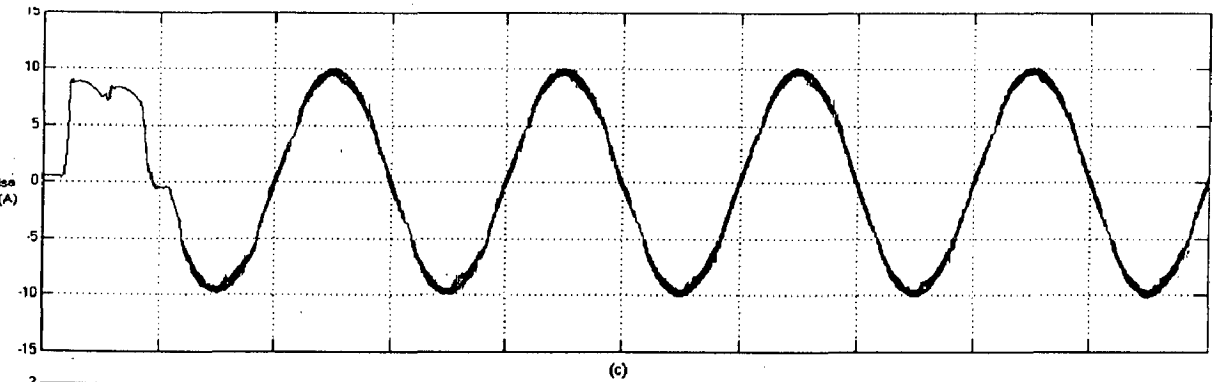
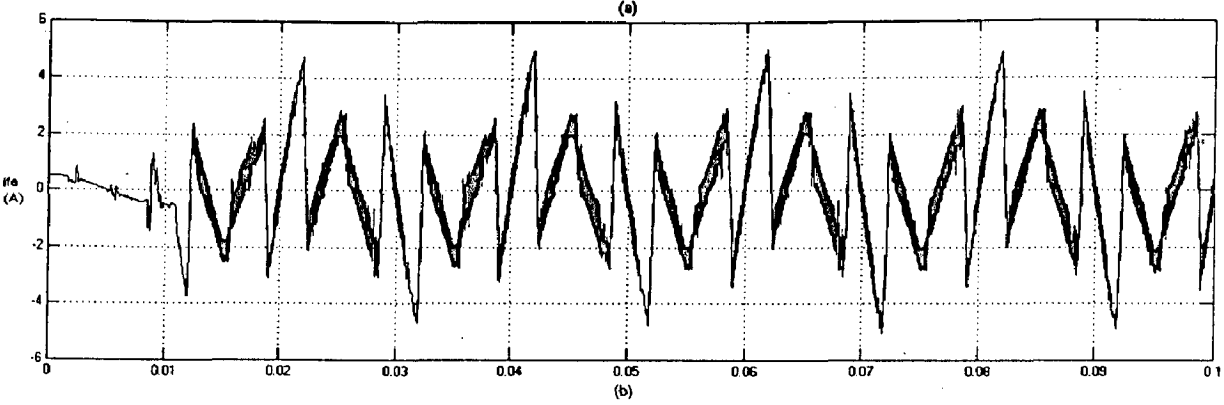
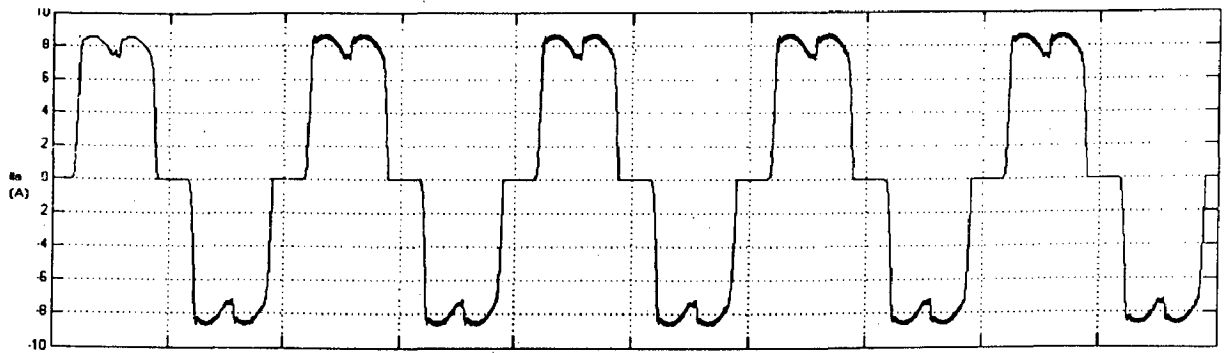


Fig. 18: (a) Load Current (A), (b) Filter Current (A), (c) Source Current (A)
 (d) Error Current (A) for RC Load

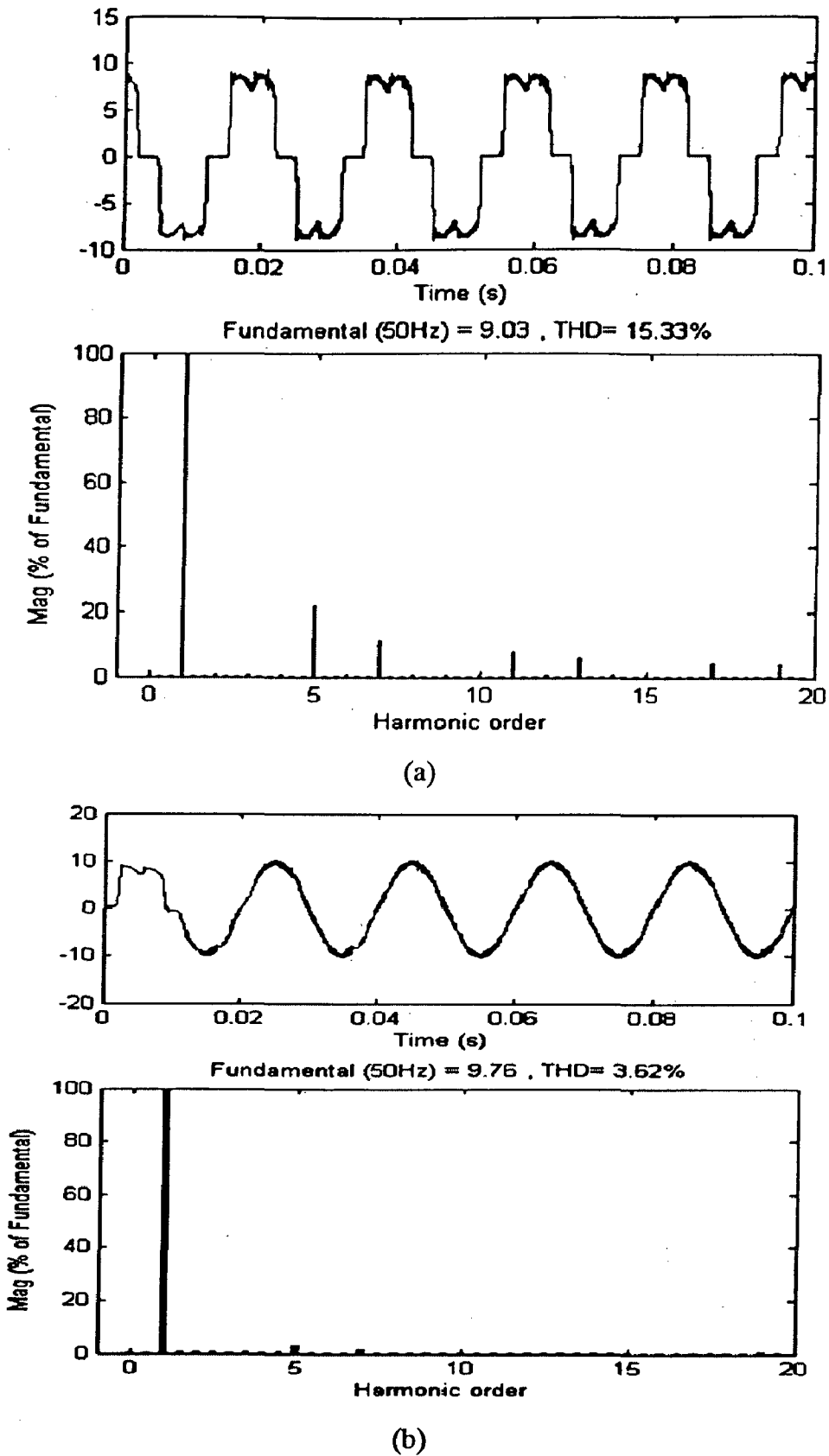


Fig. 19: FFT Analysis, (a) Load Current, (b) Source Current, for RC Load

CHAPTER-5

SPACE VECTOR MODULATED CSAPF

A lot of control schemes for PWM converters have been studied. There are sinusoidal, hysteresis, and space vector PWM controls as available techniques to control the current waveform of PWM converters. The hysteresis PWM control is simple, but its average switching frequency varies with load conditions so that switching patterns are uneven and random. In balanced three phase three wire system, the sum of instantaneous three phase current must be zero. This means that the current of one phase depends on the state of the other. Since the hysteresis and the sinusoidal PWM controls are three phase independent control, no account is taken of this phase relation in current control algorithm. On the other hand, in the space vector modulation (SVM) technique, this relation is implied in the state space vectors. The superior characteristic of the SVM technique is that the number of switching is 30 percent less than those obtained by hysteresis PWM.

5.1 Space Vector Modulation Technique

The SVM technique can be effectively implemented for both voltage source and current source inverter bridges. Let's have a brief discussion of both the schemes [10].

5.1.1 Modulation of a Voltage-Source PWM Bridge

The possible voltage vectors of the voltage-source PWM bridge are presented in Fig. 20. There are six active vectors (V1 to V6) and two zero vectors (V7 and V8). The switching combinations to produce each vector are also presented in Fig. 20, where '+' refers to upper switch and '-' to the lower switch. Sectors are labeled with Roman numerals. An ideal voltage-source bridge has simultaneously three switches in the on-state every moment. The voltage reference vector \mathbf{v}_f is produced on average during a modulation period $T_{sw}/2$ by using two active vectors. In the modulation strategy applied the two active vectors next to the reference vector and both zero vectors are used during each period. Every switching

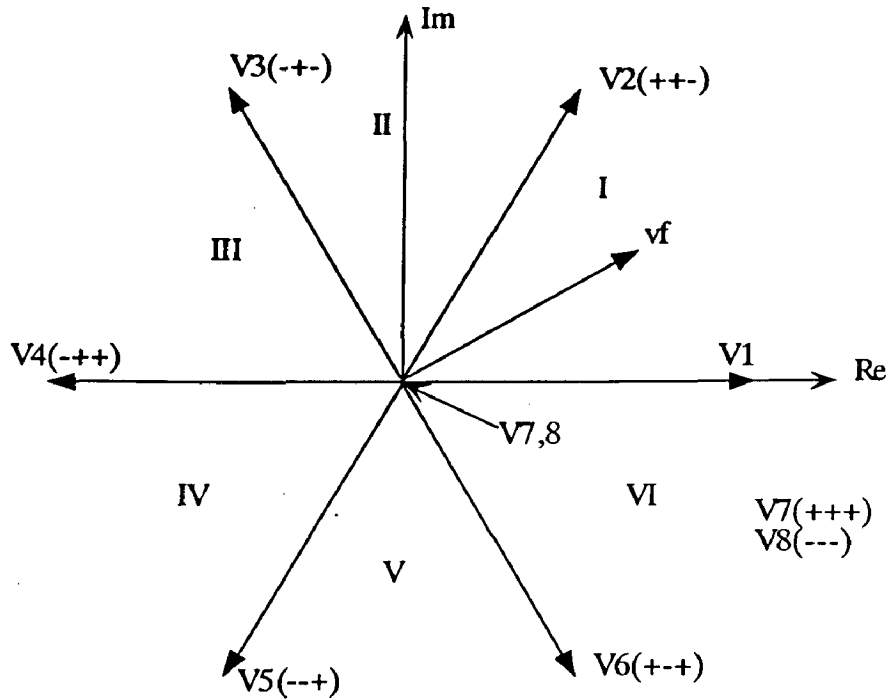


Fig.20: Space Vectors of a Voltage Source Converter

period T_{sw} begins with the zero vector V_8 and this is followed by the active vector that is adjacent to the reference vector in the sector. The active vector is chosen so that the state of switches in only one phase has to be changed at a time. After that the other active vector in the sector is applied and finally the zero vector V_7 . In the latter part of the switching period the vectors are applied in inverse sequence. It should be noted that both upper and lower switches of a phase are not allowed to be simultaneously in the on-state. To prevent the short-circuiting the dc link capacitor, in practical implementations there is a short time period between the turn-off of one of the two switching devices in a phase and the turn-on of the other device in the phase. This time is called dead time.

5.1.2 Modulation of a Current-Source PWM Bridge

The current-source PWM bridge modulates unipolar dc current. The possible current vectors of the PWM bridge are presented in Fig. 21. As with the voltage source bridge there are also six active vectors (I_1 to I_6), but in addition there are three zero vectors (I_7 to I_9). The switching combinations to produce each vector are also presented in Fig. 21. In the ideal case, the current flows through two

switching devices at the same time. The current reference vector ir^* is realized on average during a switching period T_{sw} . This is

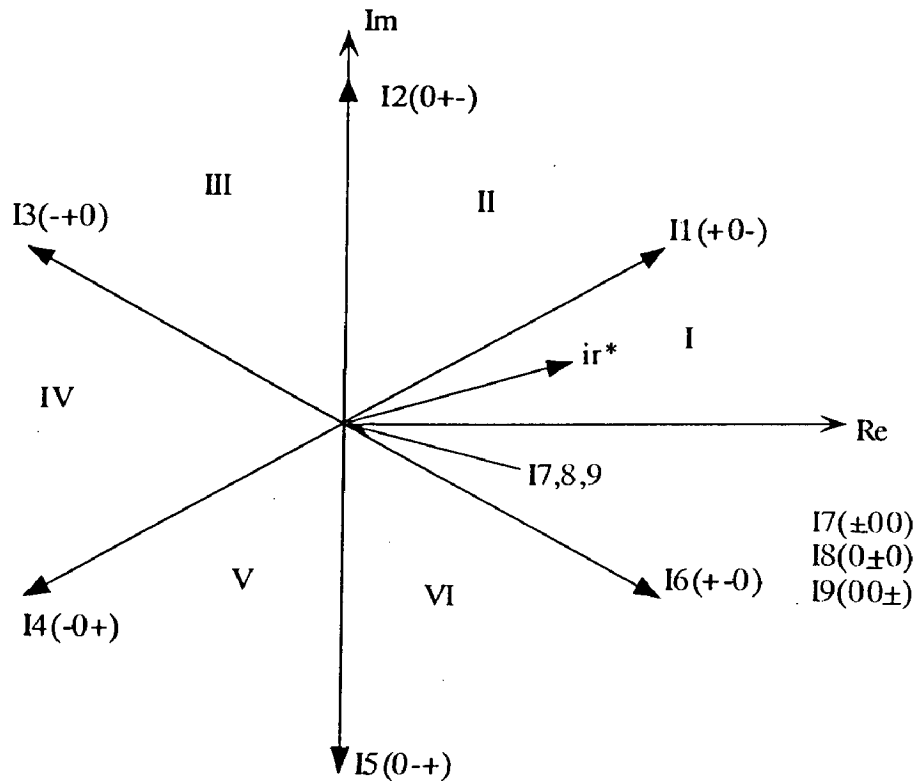


Fig.21: Space Vectors of a Current Source Converter

done using two active switching vectors. In addition one of the zero vectors is used. The '+' refers to upper switch and '-' to the lower switch while '0' indicates that neither of the switches is in on-state in a phase. The active vectors lie next to the reference vector and the zero vector is chosen so that one of the switches in the bridge is in on-state during the whole period T_{sw} . The method is called modified half wave symmetrical modulation technique. The PWM bridge may not break the dc current path. To ensure this, instead of the dead time of the voltage-source bridge, overlapping of the modulation signals is needed in practice.

5.2 SVM Implementation for CSAPF

5.2.1 Derivation of reference signals

The APF is to compensate the reactive and harmonic components of the load current so that the source current i_s may only consists of sinusoidal and in phase components with the source voltage. The compensation principle is similar as discussed with Hysteresis control in the previous chapter. The difference is that for SVM the reference current is the harmonic part of the load current (unlike the fundamental part as in Hysteresis control). Hence to compensate both the reactive power and the harmonic current, compensating powers p_c and q_c are selected as [7]:

$$\begin{aligned} p_c &= -p_{ac}^l + p_{loss} \\ q_c &= -q^l \end{aligned} \quad \dots \dots \dots 5.1$$

Where p_{loss} is the instantaneous active power corresponding to the switching loss and the resistive loss of the active power filter.

The x-y components of the compensating current is obtained as follows

$$\begin{bmatrix} i_{rx} \\ i_{ry} \end{bmatrix} = \begin{bmatrix} v_x & v_y \\ -v_y & v_x \end{bmatrix}^{-1} \begin{bmatrix} p_c \\ q_c \end{bmatrix} \quad \dots \dots \dots 5.2$$

Thus the space vector for the reference current used in the SVM technique can be obtained as

$$i_r^*(t) = i_{rx} + j i_{ry} \quad \dots \dots \dots 5.3$$

Also in polar form the reference current vector can be written as

$$i_r^*(t) = |i_r^*(t)| e^{j\theta} \quad \dots \dots \dots 5.4$$

Where

$$\begin{aligned} |i_r^*(t)| &= \sqrt{(i_{rx}^2 + i_{ry}^2)} \\ \theta &= \tan^{-1}(i_{ry} / i_{rx}) \end{aligned} \quad \dots \dots \dots 5.5$$

This compensating current is used as the reference current for the SVM technique which is discussed in the following section.

The reference current can also be obtained in three phase (a-b-c) form by the following expression

$$\begin{bmatrix} i_{ra} \\ i_{rb} \\ i_{rc} \end{bmatrix} = \begin{bmatrix} 2/3 & 0 \\ -1/3 & 1/\sqrt{3} \\ -1/3 & -1/\sqrt{3} \end{bmatrix} \begin{bmatrix} i_{rx} \\ i_{ry} \end{bmatrix} \dots\dots\dots 5.6$$

5.2.2 Generation of Switching Functions

The main circuit of the PWM rectifier is shown in Fig. 10. This PWM rectifier uses six unidirectional switches to connect the three-phase source to the load. The switching function for a switch S_k ($k=1, 2 \dots 6$) is defined as [9]:

$$d_k^* = 1 \quad \text{when switch } S_k \text{ is on}$$

$$d_k^* = 0 \quad \text{when switch } S_k \text{ is off}$$

Because two switches in two different legs-one in the upper switch bridge (S_1, S_3, S_5) and the other in the lower switch bridge (S_4, S_6, S_2) are allowed to conduct in any moment, the following relations are satisfied:

$$d_1^* + d_3^* + d_5^* = 1$$

$$d_4^* + d_6^* + d_2^* = 1 \quad \dots\dots\dots 5.7$$

It is assumed that the output current is constant during the switching period T , due to the sufficiently large filter inductance while the output voltage of the PWM rectifier is not necessarily constant. The line current of the PWM rectifier is then given by

$$i_{ra} = (d_1^* - d_4^*)I$$

$$i_{rb} = (d_3^* - d_6^*)I \quad \dots\dots\dots 5.8$$

$$i_{rc} = (d_5^* - d_2^*)I$$

The rectifier can produce only six space vectors (**I1** to **I6**) and three zero vectors of the current (**I7** to **I9**), shown in Table I. The quantized space vectors of the current are obtained as follows:

$$I_n = 2/3 I e^{j(2n-1)\pi/6} \quad \text{for } n = 1, 2 \dots \dots 6$$

$$\dots\dots\dots 5.9$$

$$I_n = 0 \quad \text{for } n = 7, 8, 9.$$

TABLE III
Switching Combinations of the Current Source PWM inverter

| | I1 | I2 | I3 | I4 | I5 | I6 | I7 | I8 | I9 |
|-----------|-----------|-----------|-----------|-----------|-----------|-----------|-----------|-----------|-----------|
| S1 | 1 | 0 | 0 | 0 | 0 | 1 | 1 | 0 | 0 |
| S2 | 1 | 1 | 0 | 0 | 0 | 0 | 0 | 0 | 1 |
| S3 | 0 | 1 | 1 | 0 | 0 | 0 | 0 | 1 | 0 |
| S4 | 0 | 0 | 1 | 1 | 0 | 0 | 1 | 0 | 0 |
| S5 | 0 | 0 | 0 | 1 | 1 | 0 | 0 | 0 | 1 |
| S6 | 0 | 0 | 0 | 0 | 1 | 1 | 0 | 1 | 0 |

Current vectors **I7**, **I8** and **I9**, give zero voltage of the PWM inverter and at this condition the input current $i_r(t)$ of the PWM rectifier is also zero. The space vector $i_r(t)$ of the current can be expressed by combining the space vectors in 5.9. To obtain the required space vector $i_r(t)$ the conduction times of the rectifier switches are modulated according to the amplitude and angle of $i_r(t)$. The angle of $i_r(t)$ determines the sector of the complex plane. The required space vector $i_r(t)$ is modulated as follows:

$$i_r(t) = \frac{(T_a I_a + T_b I_b)}{T_s} \dots \dots \dots 5.10$$

This is defined as space vector modulation. This modulation is achieved by using two adjacent space vectors I_a and I_b , with the appropriate duty cycle T_a and T_b denote the on time of the space vectors I_a , and I_b , respectively. The real and imaginary components of $i_r(t)$ in the above equation are denoted as

$$i_r(t) = \frac{2}{\sqrt{3}} I \left[\left(T_a + \frac{T_b}{2} \right) + j \frac{\sqrt{3}}{2} T_b \right] \dots \dots \dots 5.11$$

From Fig. 22, the real and imaginary components of $i_r(t)$ can be also given by

$$i_r(t) = \left(i_{ra} + \frac{i_{rb}}{2} \right) + j \frac{\sqrt{3}}{2} i_{rb} \dots \dots \dots 5.12$$

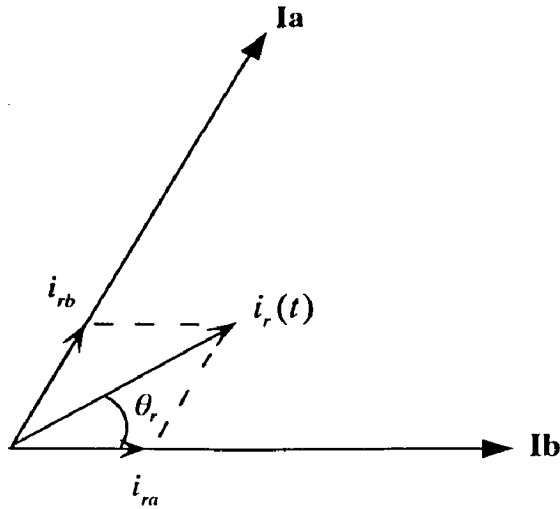


Fig. 22: Current Components

$$i_{ra} = \frac{2}{\sqrt{3}} |i_r(t)| \sin\left(\frac{\pi}{3} - \theta_r\right) \dots\dots\dots 5.13$$

$$i_{rb} = \frac{2}{\sqrt{3}} |i_r(t)| \sin \theta_r$$

Where

$|i_r(t)|$ and θ_r denote the magnitude and location of the space vector $i_r(t)$ respectively.

$$|i_r(t)| = \sqrt{(\text{Re}\{i_r(t)\})^2 + (\text{Im}\{i_r(t)\})^2}$$

$$\theta_r = \frac{n\pi}{3} - \tan^{-1}\left(\frac{\text{Im}\{i_r(t)\}}{\text{Re}\{i_r(t)\}}\right) + \frac{\pi}{6}$$

Where n is the sector number. Comparing 5.12 to 5.13, the on time T_a and T_b , of two adjacent space vectors **Ia** and **Ib** are given by

$$T_a = \frac{|i_r(t)|}{I} T_s \sin\left(\frac{\pi}{3} - \theta_r\right) \dots\dots\dots 5.14$$

$$T_b = \frac{|i_r(t)|}{I} T_s \sin \theta_r$$

Then, the on time T_0 of the zero vector is

$$T_0 = T_s - T_a - T_b \dots\dots\dots 5.15$$

From conditions given in the above three equations, switching functions of the switches in the sector $n = 1$ are obtained as follows:

$$\begin{aligned}
d_1 &= 1 \\
d_3 &= d_5 = 0 \\
d_6 &= m \sin\left(\frac{\pi}{3} - \theta_r\right) \dots\dots\dots 5.16 \\
d_2 &= m \sin \theta_r \\
d_4 &= 1 - d_6 - d_2
\end{aligned}$$

Where the modulation index m ($0 < m < 1$) is defined as:

$$m = \frac{|i_r(t)|}{I} \dots\dots\dots 5.17$$

Since these switching functions are positive for the full range of θ_r , they are implement- able. Table IV shows the switching functions of the six switching in all sectors. It is very difficult to implement these switching functions using conventional sinusoidal PWM control.

TABLE IV
SWITCHING FUNCTIONS OF THE SIX SWITCHES

| | n = 1 | n = 2 | n = 3 | n = 4 | n = 5 | n = 6 |
|-----------|---|---|---|---|---|---|
| d1 | 1 | $m \sin\left(\frac{\pi}{3} - \theta_r\right)$ | 0 | 1-d3-d5 | 0 | $m \sin \theta_r$ |
| d2 | $m \sin \theta_r$ | 1 | $m \sin\left(\frac{\pi}{3} - \theta_r\right)$ | 0 | 1-d4-d6 | 0 |
| d3 | 0 | $m \sin \theta_r$ | 1 | $m \sin\left(\frac{\pi}{3} - \theta_r\right)$ | 0 | 1-d5-d1 |
| d4 | 1-d6-d2 | 0 | $m \sin \theta_r$ | 1 | $m \sin\left(\frac{\pi}{3} - \theta_r\right)$ | 0 |
| d5 | 0 | 1-d1-d3 | 0 | $m \sin \theta_r$ | 1 | $m \sin\left(\frac{\pi}{3} - \theta_r\right)$ |
| d6 | $m \sin\left(\frac{\pi}{3} - \theta_r\right)$ | 0 | 1-d2-d4 | 0 | $m \sin \theta_r$ | 1 |

5.2.3 PWM Pattern Generation

The switching are so selected as to minimize the switching loss. In the sector $n = 1$, it should be noted that switch S1 remains ON state for all the time. The constraints make the others to be selected in the lower leg. For a particular sample period T_s , the switches S6 and S2 of lower leg are selected for the switching functions d_6 and d_2 respectively. The conducting time of the switches are distributed in the switching period with no overlap. The remaining switch of the lower leg should be the compliment to S1. Thus S4 is selected for the switching function d_4 . it should be noted that the other switches of the upper leg, i.e., S3 and S5 will not turn on in sector $n = 1$.

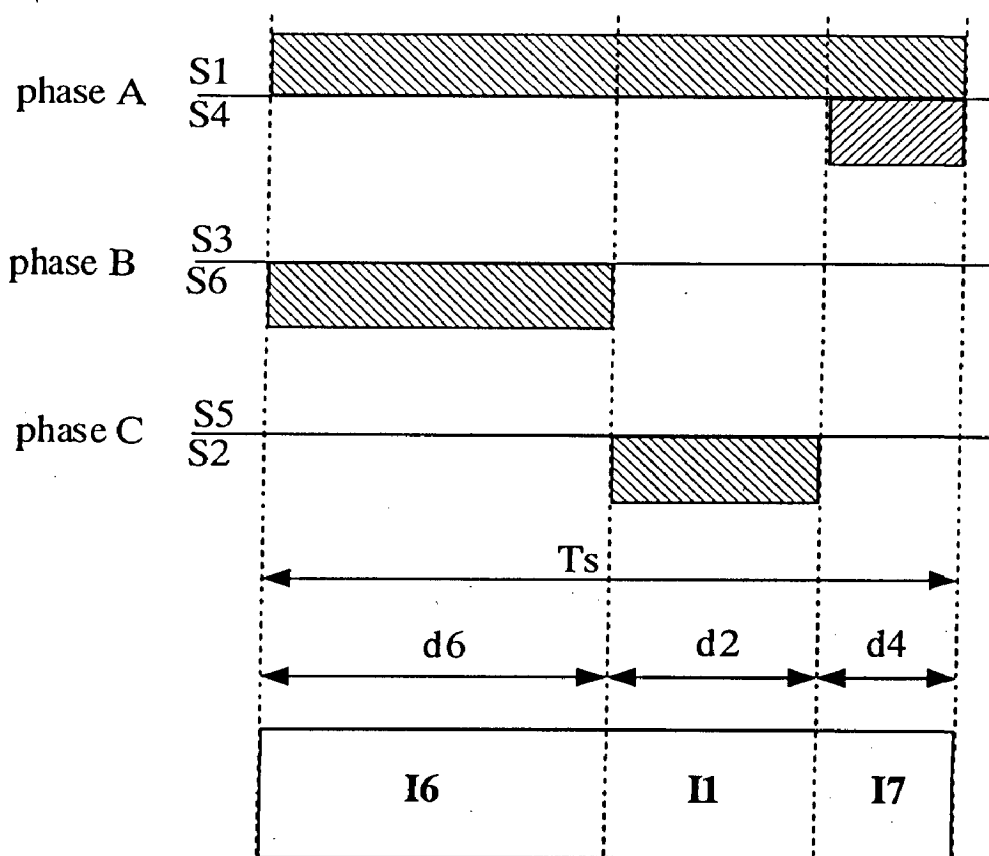


Fig. 23: PWM patterns for CSAPF

This concept can be directly applied for all sectors. Table II shows the switching functions of the six switches in all sectors. These functions will be useful when the desired phase current vector $i_r(t)$ of converter is given in complex form.

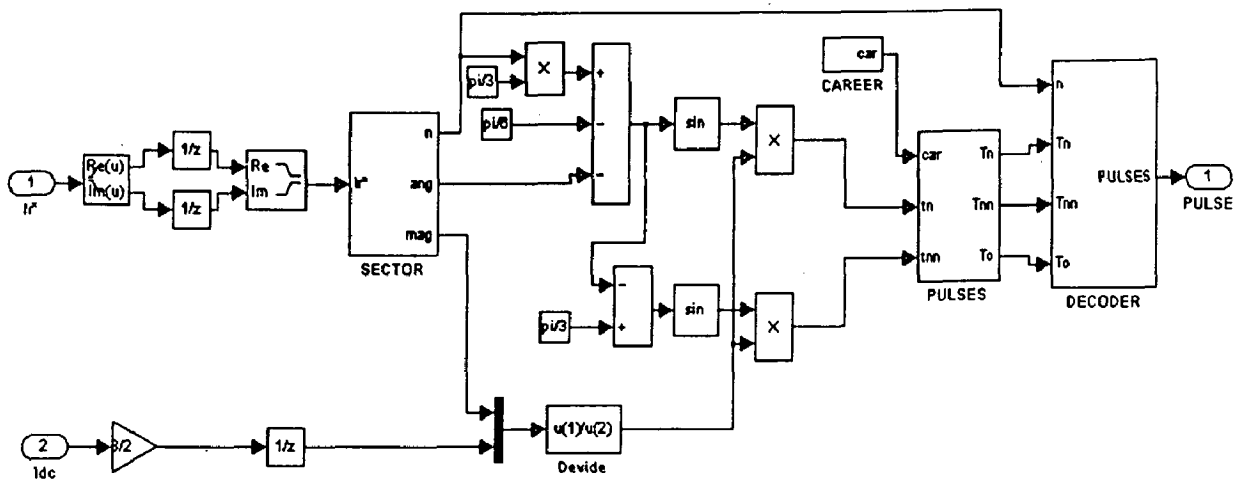


Fig. 25: Simulink Model for the Subsystem for the Space Vector Modulation

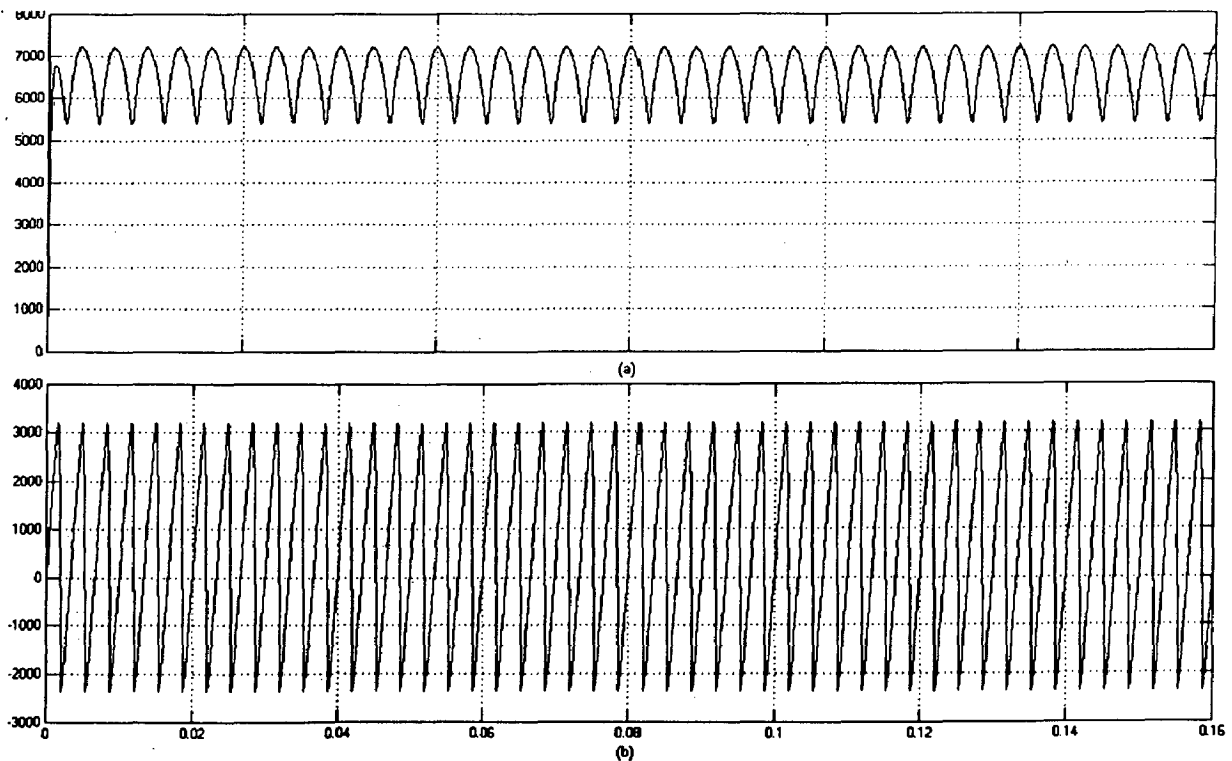


Fig. 26: Instantaneous power drawn from source by the diode bridge RL load
 (a) Instantaneous active power (W), (b) Instantaneous reactive power (VAR)

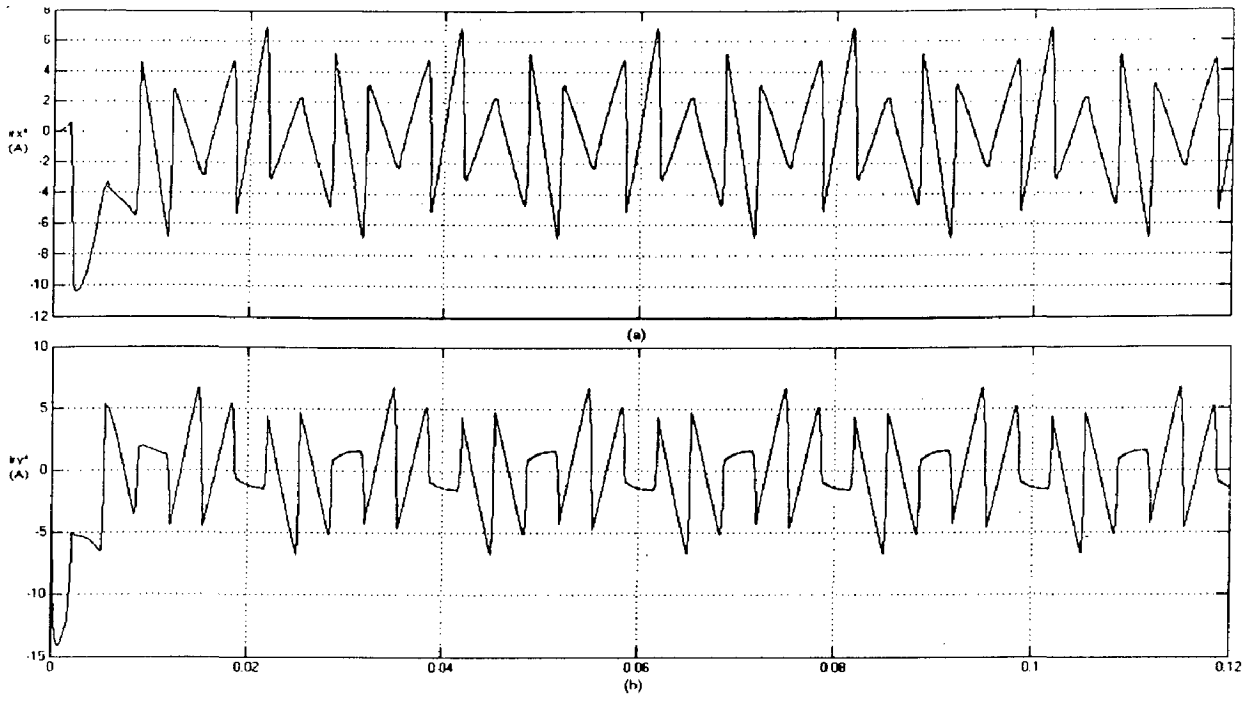


Fig. 27: Orthogonal Components for Reference Current
 (a) x-component, (b) y-component

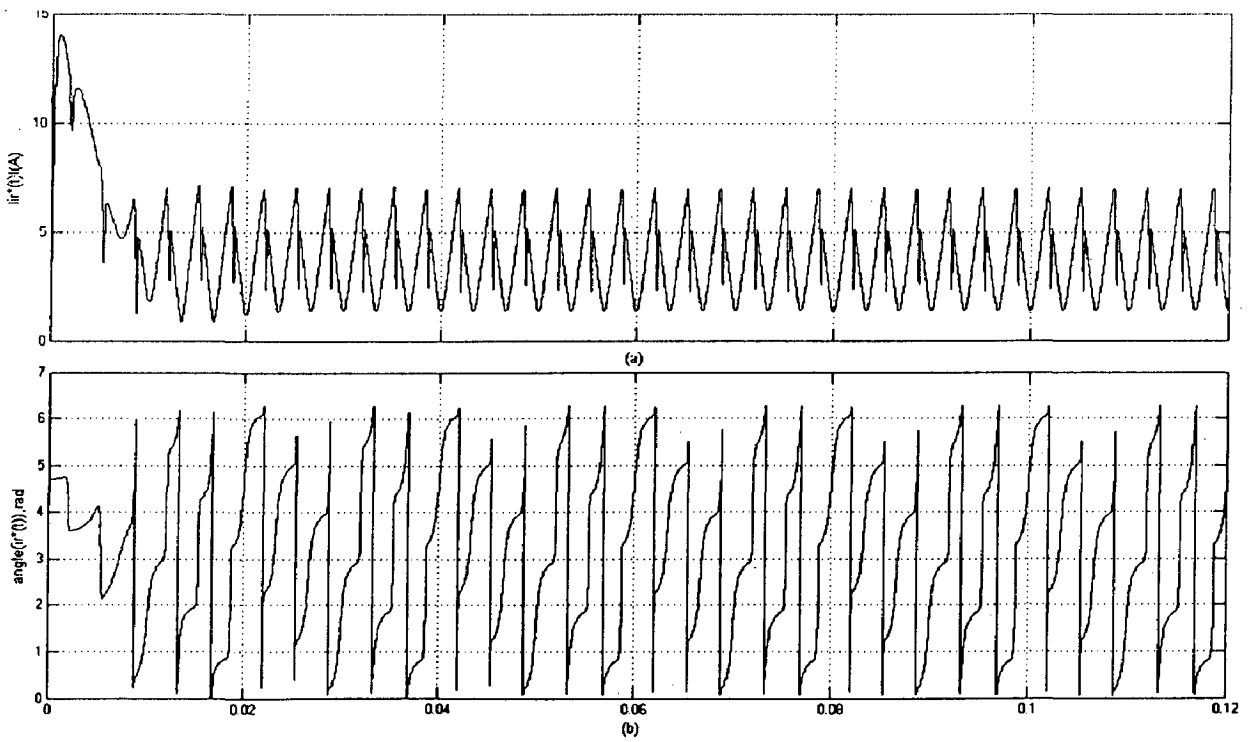


Fig. 28: Reference Current in polar form
 (a) Magnitude (A), (b) angle (rads)

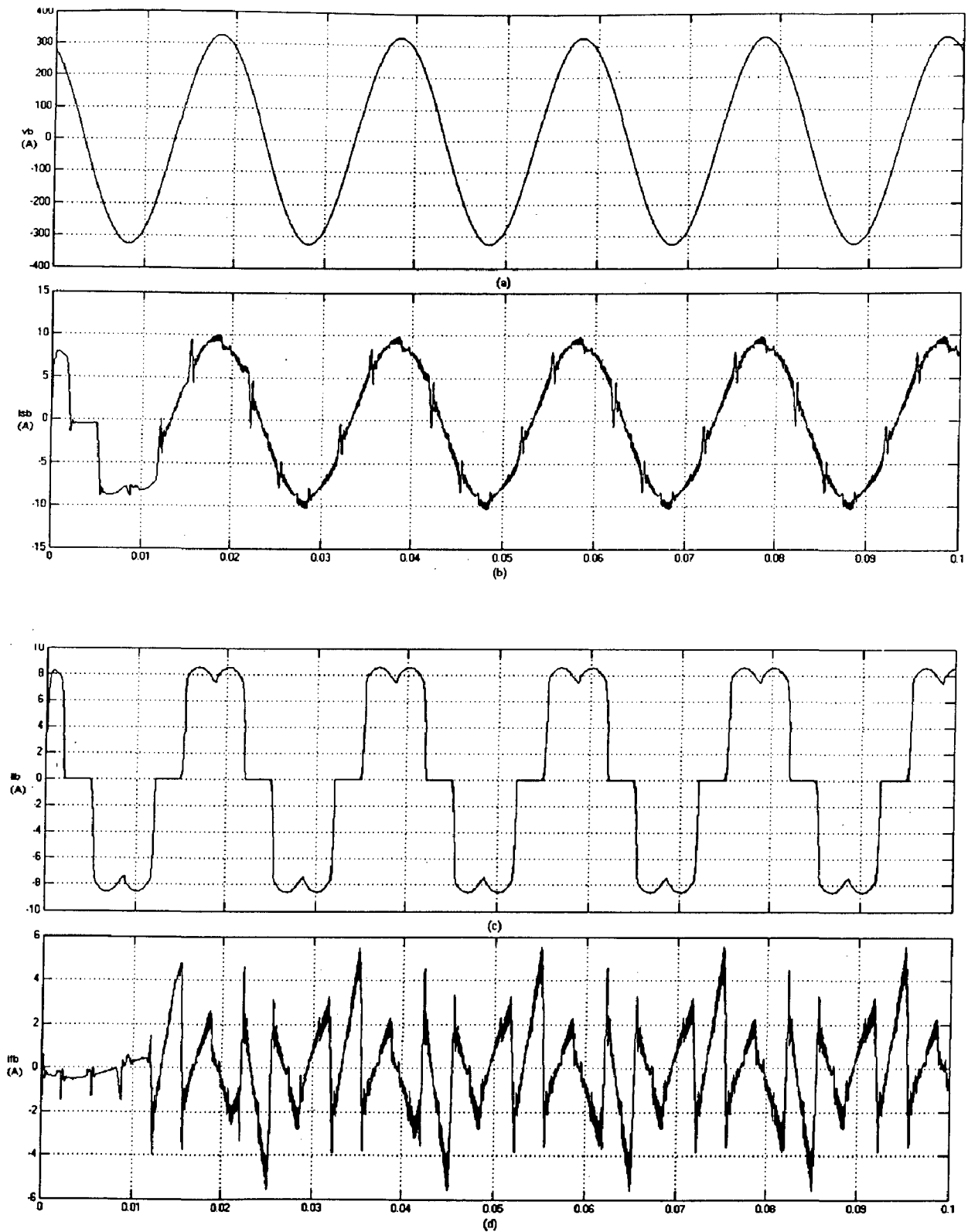


Fig. 29: (a) Source Voltage (V), (b) Source Current (A), (c) Load Current (A),
(d) Filter Current (A) for RL Load

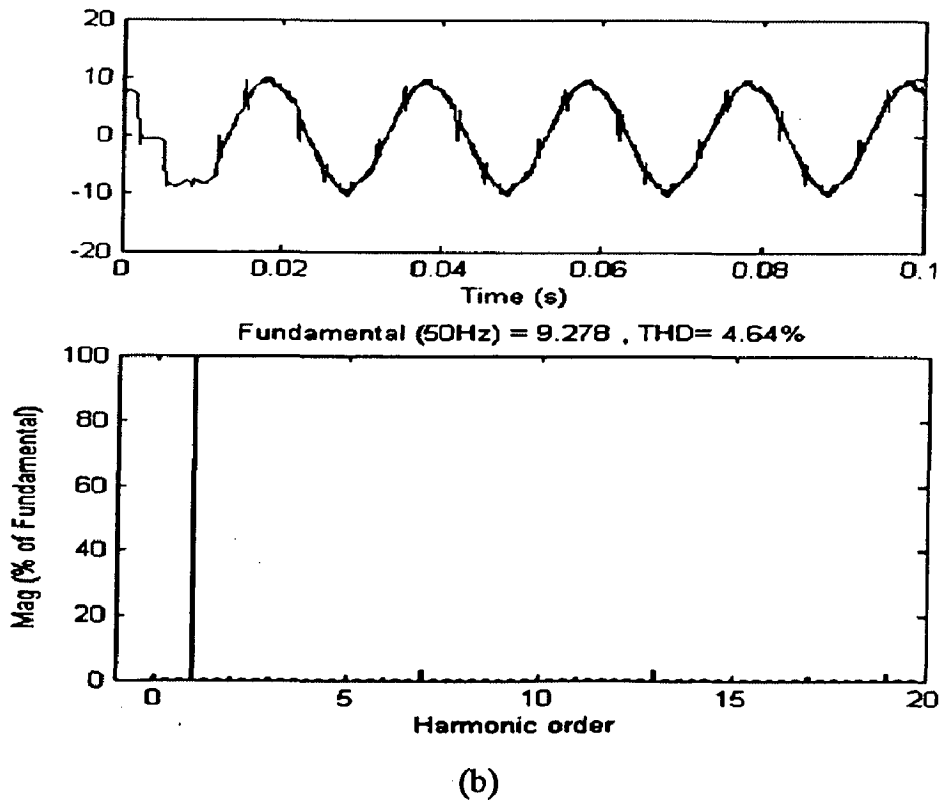
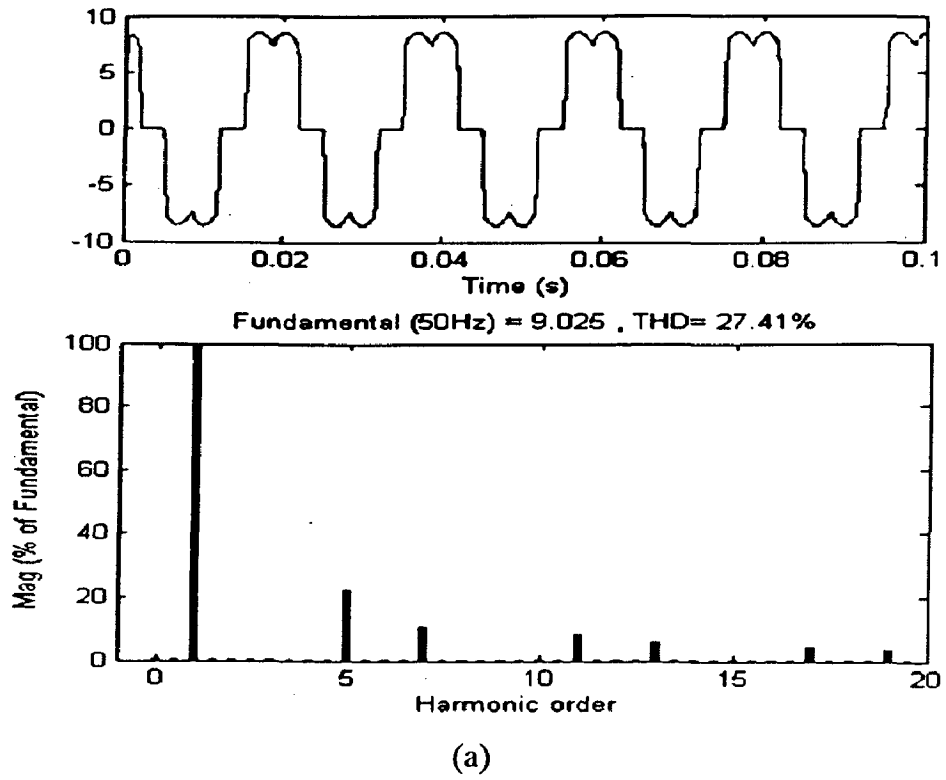


Fig. 30: FFT Analysis, (a) Load Current, (b) Source Current, for RL Load

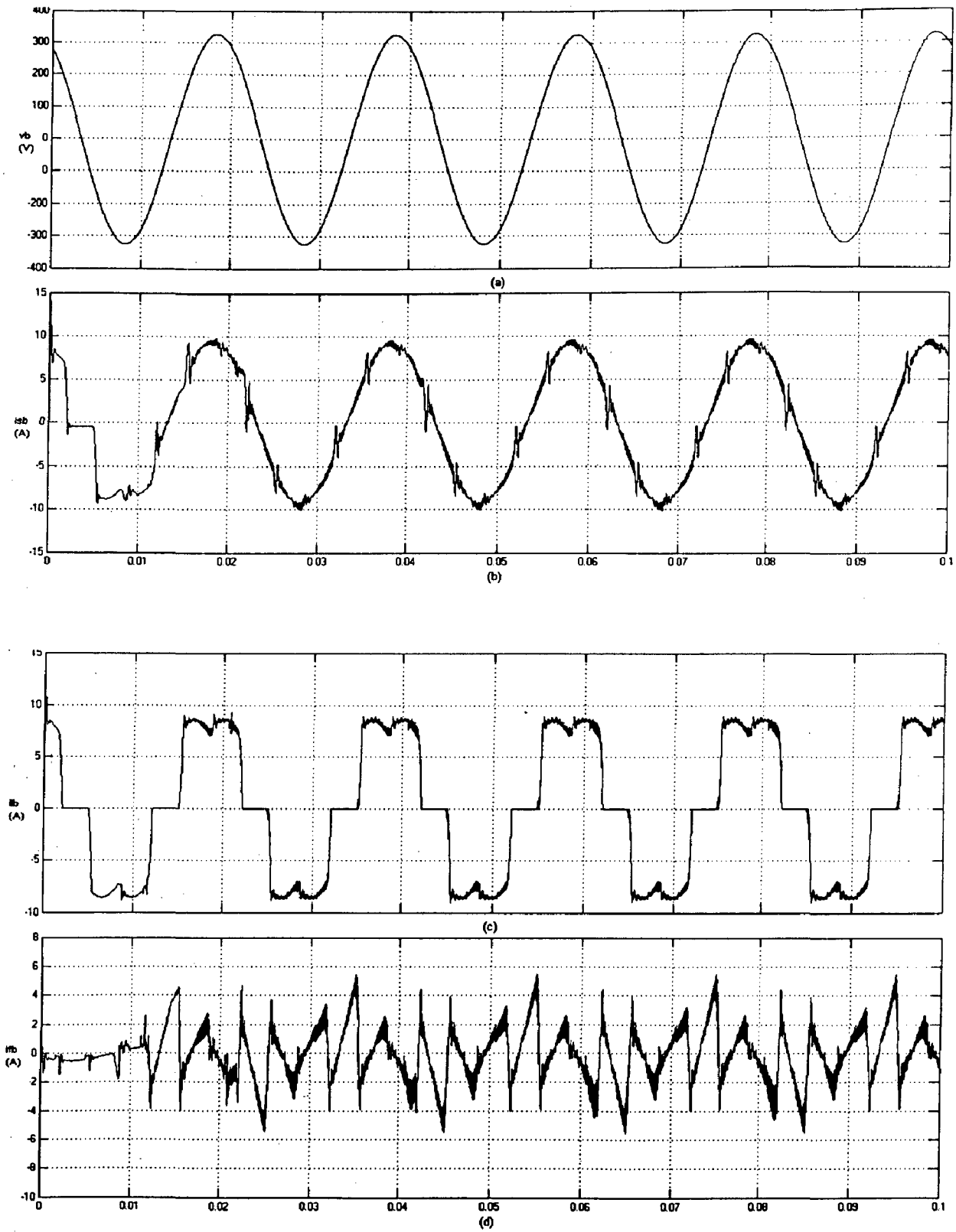


Fig. 31: (a) Source Voltage (V), (b) Source Current (A), (c) Load Current (A),
 (d) Filter Current (A) for RC Load

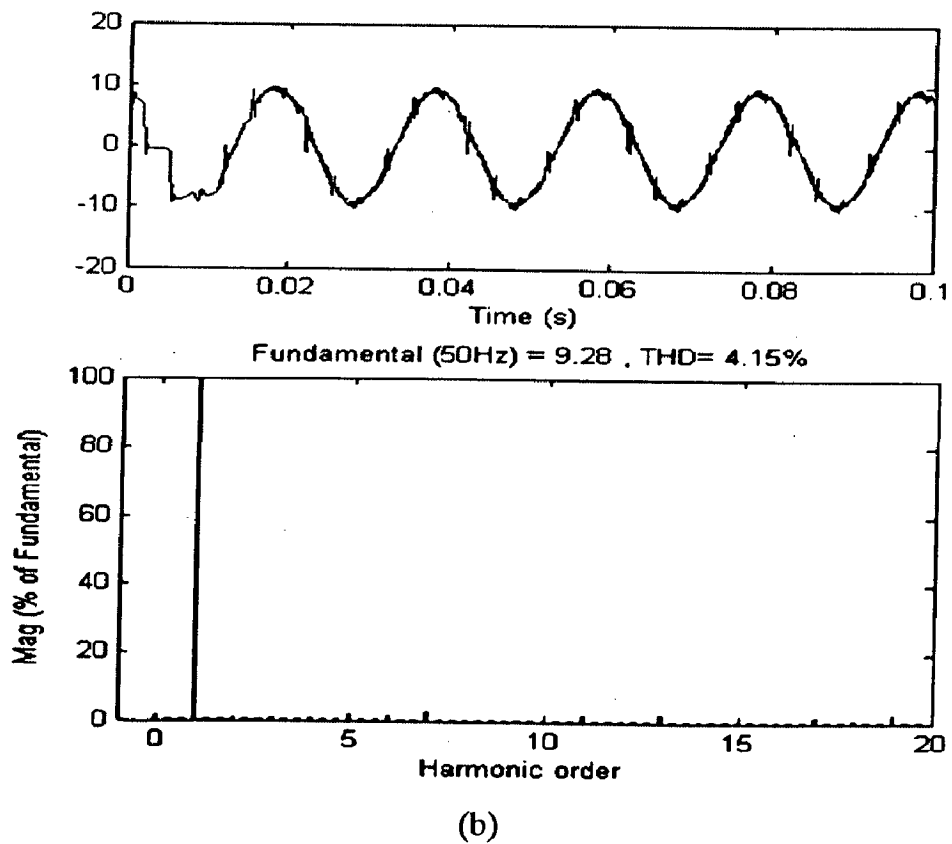
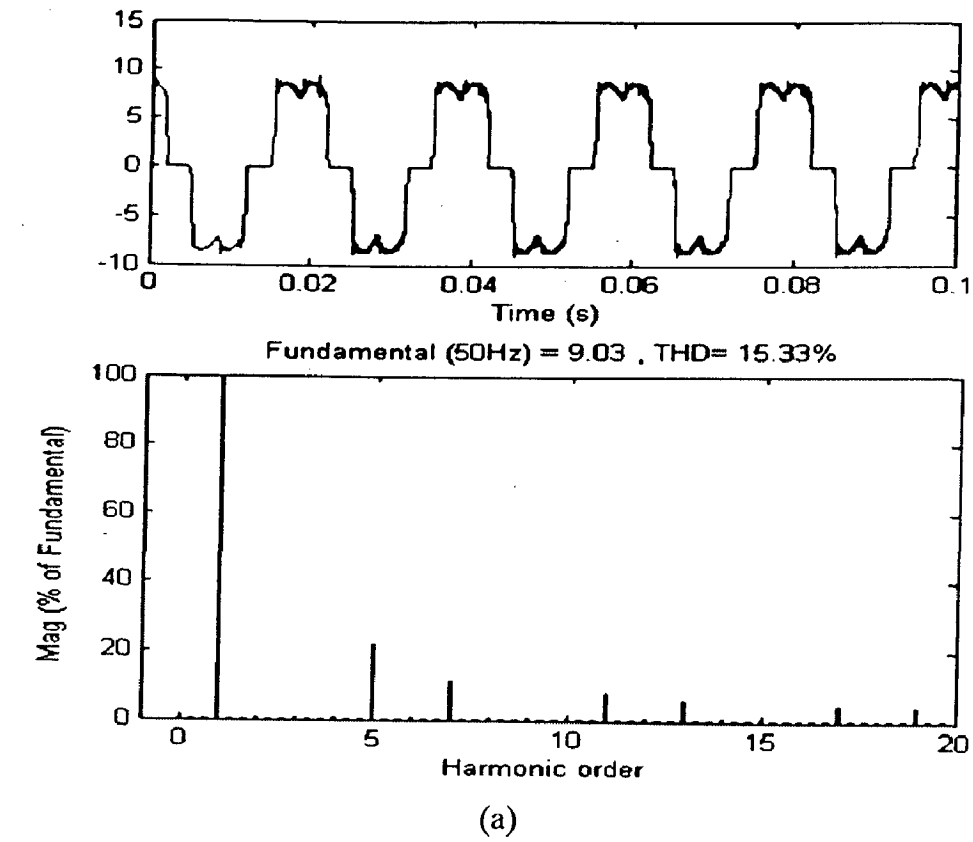


Fig. 32: FFT Analysis, (a) Load Current, (b) Source Current, for RC Load

CHAPTER-6

ARTIFICIAL NEURAL NETWORKS

Artificial neural networks are very often compared with human brain system. Fig. 33 shows an extremely simplified model of the brain. A neural network system essentially works as a function approximator, very much like a human brain. It transforms inputs into outputs to the best of its ability. Moreover it has the ability to learn from its past experiences.

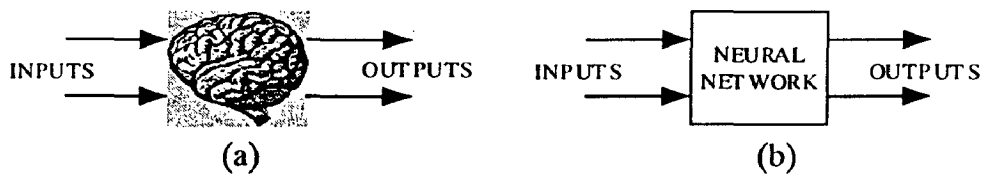


Fig. 33: Simplified Model of (a) Brain, (b) Neural Network

The main features of neural network are

- Ability to learn
NN's figure out how to perform their function on their own
Determine their function based only upon sample inputs
- Ability to generalize
Produce reasonable outputs for inputs it has not been taught how to deal

with

The neural networks are used for the following purposes to serve:

- Classification
Pattern recognition, feature extraction, image matching
- Noise Reduction
Recognize patterns in the inputs and produce noiseless outputs
- Prediction
Extrapolation based on historical data



6.1 Neuron Model

Simplified model of a single neuron is shown in Fig. 34. The output of a neuron is a function of the weighted sum of the inputs plus a bias. The function of the entire neural network is simply the computation of the outputs of all the neurons. It is an entirely deterministic calculation.

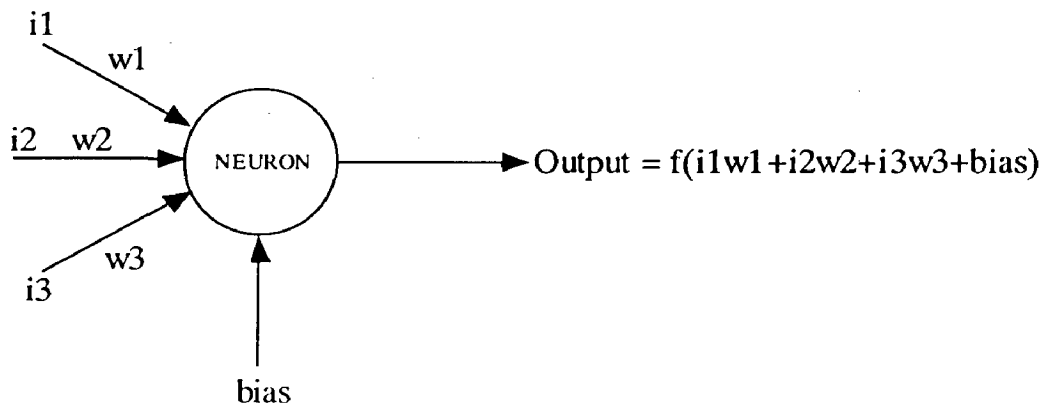


Fig. 34: Single Neuron Model

An activation function is applied to the weighted sum of the inputs of a neuron to produce the output. Majority of NN's use sigmoid functions like logistic function, hyperbolic function and arctangent. The exact nature of the function has little effect on the abilities of the neural network.

Each input is assigned with a weight which can be modified by training the network. The weights in a neural network are the most important factor in determining its function. Training is the act of presenting the network with some sample data and modifying the weights to better approximate the desired function.

There are two main types of training

- Supervised Training

It supplies the neural network with inputs and the desired outputs. The weights are modified to reduce the difference between the actual and desired outputs.

- Unsupervised Training

It only supplies inputs. The network identifies the patterns and differences in

the inputs without any external assistance.

6.2 Perceptrons

A single layer perceptron is the most fundamental neural network which has the ability to learn. It is made up of only input neurons and output neurons. Input neurons typically have two states: ON and OFF. Output neurons use a simple threshold activation function. It uses supervised training for learning in basic form, can only solve linear problems.

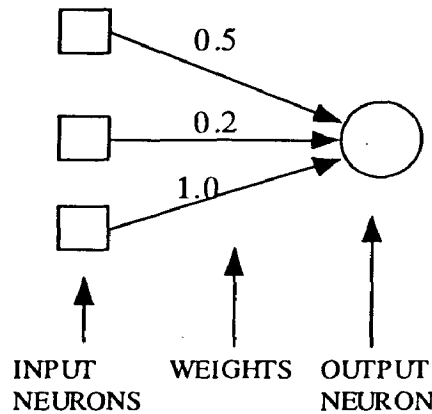


Fig. 35: Single Layer Perceptron

Most common neural network is the multilayer perceptron. It is an extension of the single layer perceptron. In Multiple layers there are the additional of one or more “hidden” layers in between the input and output layers. Information flows in one direction, i.e., the outputs of one layer act as inputs to the next layer.

6.3 Back propagation Networks

Back propagation is the method of calculation of the derivatives flows backwards through the network, hence the name, back propagation. These derivatives point in the direction of the maximum increase of the error function. A small step (learning rate) in the opposite direction will result in the maximum decrease of the (local) error function:

$$W_{new} = W_{old} + \alpha \frac{\partial E}{\partial W_{old}} \quad \dots \dots \dots 6.1$$

Where E is the error function and α is the learning rate.

The learning rate is an important factor. If it is too small, the system convergence becomes extremely slow and if it is too large then the system may not converge.

6.4 Counter propagation Neural Networks (CPNN)

It is another type of multilayer feed forward network. The special feature of this network is that it is up to 100 times faster than back propagation. But it is not as general as back propagation. The network is made up of three layers:

- Input layer
- Hidden layer
- Output layer

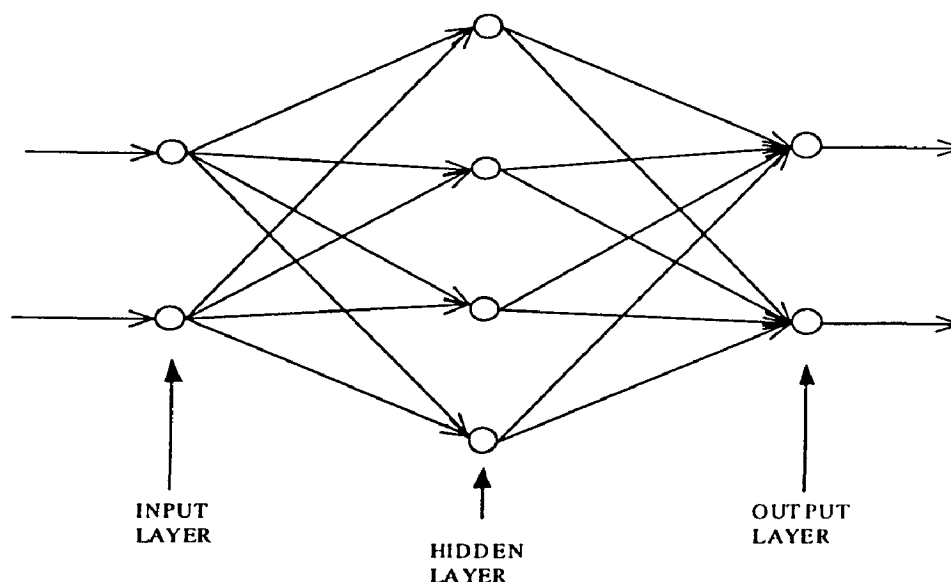


Fig. 36: Counter propagation Neural Networks (CPNN)

For the multi-layer structure it is more accurate representation of biological neural networks. Each layer has its own distinct purpose:

- Hidden layer separates inputs into separate classes. Inputs in the same class will turn on the same neuron of the layer
- Output layer adjusts weights to obtain acceptable outputs for each class

An important use of counter propagation learning networks is found in vector quantization. A vector quantization scheme divides the input space in a number of disjoint subspaces and represents each input vector by the label of the subspace it falls into. The quantization performed by the competitive learning network is said to 'track the input probability density function': the density of neurons and thus subspaces is highest in those areas where inputs are most likely to appear, whereas a more coarse quantization is obtained in those areas where inputs are scarce.

CHAPTER-7

ANN APPROACH TO SVM IMPLEMENTATION FOR CSAPF

The rapid development of the switching frequency capabilities of power semiconductor devices requires faster, more accurate and simpler modulation techniques. Among the different PWM techniques available, the Space Vector Modulation (SVM) has become the preferred method for digital implementations in three-phase converters. Although implementation of the SVM technique in digital systems is in principle simple, the required calculations and corresponding execution times limit the minimum sampling time. Thus, there is a maximum switching frequency attainable, and the maximum bandwidth of the overall control system is limited. By exploiting the concept of vector classification used in the so called instar competitive layer of a counter propagation neural network (CPN competitive layer), the hardware and software complexity of the implementation of the SVM can be considerably reduced. Such an implementation is proposed here. It requires less hardware and less computational effort. Therefore, the required sampling time can be reduced and thereby, higher switching frequencies can be achieved compared with conventional SVM implementations.

7.1 Proposed Network

Because, the SVM is a deterministic problem and all classes are known in advance, there is no need to train a neural network. In addition, the signal processing technique employed in this paper is slightly different from the one used in CPN. The instar hidden layer of the CPN comprises a set of processing elements known as instars. The instar is a single processing element that shares its general structure and processing functions with other processing elements. The training procedure of the traditional CPN competitive layer is described below. Given a set of input vectors to be classified into a specific number of classes, the numbers of instars (neurons) in the hidden layer are selected to be equal to the number of the desired classes. The normalized input vectors are then applied to the input layer, and pre-

randomly selected weights are adjusted to give the closest vector to a class of clusters. After the training process, when a normalized input vector appears at the input layer of the network, the net input of each instar is the inner product between the input vector and the associated weight vector. Thus, the net input after training represents one class of input vectors. In other words:

$$net = U.W = \|U\| \|W\| \cos \theta \quad \dots \dots \dots 7.1$$

Since the input vector and the weight vector are normalized, the instars net input (shown in above equation) gives the cosine of the angles between the input vector and the weight vectors that represent the classes. The largest instar net input wins the competition and the input vector is then classified in that class. This procedure after training is shown in Fig. 37.

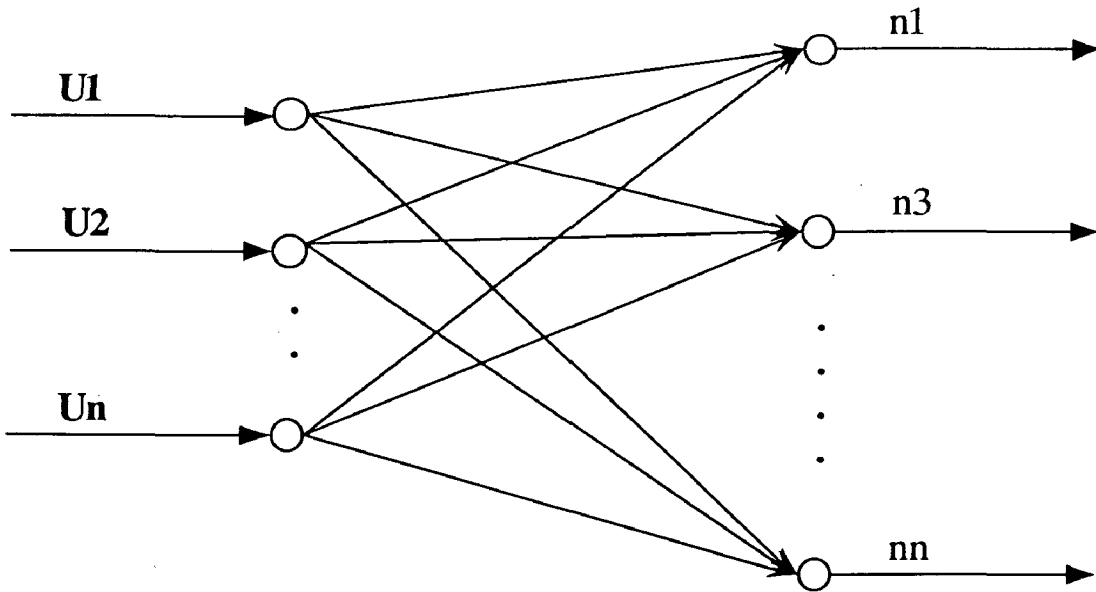


Fig. 37: A layer of neurons arranged in competitive layer

It is a layer of instars arranged in competitive layer. Each unit receives the input vector $U = [U_1, U_2, \dots, U_n]^T$ and the i th unit has associated with it the weight vector, $W_i = [W_{i1}, W_{i2}, \dots, W_{in}]^T$. Net input values are calculated in the $net\ n_i = U.W_i$. The winners of the competition are the units corresponding to the classes where the input vector lies.

SVM is fundamentally a classification problem. The classes are known in advance, and there is no need to train the network. By its very nature, the SVM technique requires that the sector, where the input vector lies be specified. To do this, the

borders should be known, thus the competitive layer must have two winners. The on-time interval of each switch thereafter can be obtained by applying another simple signal processing to the winner net inputs. This leads to another modification consisting of simply setting the output of winners equal to their net inputs (in conventional CPN the winner is set to one, and the rest are set to zero). The whole procedure therefore can be explained as follows.

7.2 Calculation Method

The expressions for the on-time intervals of a current source converter can be calculated in the following way [12]. The reference current can also be obtained in three phase (a-b-c) form by the following expression

$$\begin{bmatrix} i_{ra} \\ i_{rb} \\ i_{rc} \end{bmatrix} = \begin{bmatrix} 2/3 & 0 \\ -1/3 & 1/\sqrt{3} \\ -1/3 & -1/\sqrt{3} \end{bmatrix} \begin{bmatrix} i_{rx} \\ i_{ry} \end{bmatrix} \dots\dots\dots 7.2$$

The nets can be found from the reference current as follows:

$$\begin{aligned} n_1 &= i_{ra} - i_{rc}, n_2 = i_{rb} - i_{rc}, n_3 = i_{rb} - i_{ra} \\ n_4 &= -n_1, n_5 = -n_2, n_6 = -n_3 \end{aligned} \dots\dots\dots 7.3$$

Combining above two equations the inner product of 7.1 in the matrix form can be changed to:

$$\begin{bmatrix} n_1 \\ n_2 \\ n_3 \\ n_4 \\ n_5 \\ n_6 \end{bmatrix} = \begin{bmatrix} 1 & \frac{1}{\sqrt{3}} \\ 0 & \frac{2}{\sqrt{3}} \\ -1 & \frac{1}{\sqrt{3}} \\ -1 & -\frac{1}{\sqrt{3}} \\ 0 & -\frac{2}{\sqrt{3}} \\ 1 & -\frac{1}{\sqrt{3}} \end{bmatrix} \begin{bmatrix} i_{rx} \\ i_{ry} \end{bmatrix} \dots\dots\dots 7.4$$

The above equation is compared with 7.1, and thereby the weight matrix and input vectors associated with CPN competitive layer are obtained.

$$W = \begin{bmatrix} 1 & 0 & -1 & -1 & 0 & 1 \\ \frac{1}{\sqrt{3}} & \frac{2}{\sqrt{3}} & \frac{1}{\sqrt{3}} & -\frac{1}{\sqrt{3}} & -\frac{2}{\sqrt{3}} & -\frac{1}{\sqrt{3}} \end{bmatrix}^T, \quad U = \begin{bmatrix} i_x \\ i_y \end{bmatrix} \quad \dots\dots 7.5$$

The above equation shows that the inner product between the reference and a space vector is a simple linear combination of the two current references. Since the last three rows of the weight matrix are simply the negative of the first three rows, less computational effort is required if efficient programming is used.

Assume a specific $i_r(t)$ is applied to the competitive layer, n_i and n_j are the neurons who win the competition. According to 7.1 we have:

$$\begin{bmatrix} n_i \\ n_j \end{bmatrix} = \sqrt{3} \|i_r(t)\| \begin{bmatrix} \cos\left(\frac{\pi}{3} - \theta\right) \\ \cos\theta \end{bmatrix} \quad \dots\dots\dots 7.6$$

But

$$\begin{bmatrix} \cos\left(\frac{\pi}{3} - \theta\right) \\ \cos\theta \end{bmatrix} = \frac{2}{\sqrt{3}} \begin{bmatrix} 1 & \frac{1}{2} \\ \frac{1}{2} & 1 \end{bmatrix} \begin{bmatrix} \sin\left(\frac{\pi}{3} - \theta\right) \\ \sin\theta \end{bmatrix} \quad \dots\dots\dots 7.7$$

Combining above two equations, we have

$$\begin{bmatrix} n_i \\ n_j \end{bmatrix} = \sqrt{3} \|i_r(t)\| \frac{T}{I} \frac{2}{\sqrt{3}} \begin{bmatrix} 1 & \frac{1}{2} \\ \frac{1}{2} & 1 \end{bmatrix} \begin{bmatrix} \sin\left(\frac{\pi}{3} - \theta\right) \\ \sin\theta \end{bmatrix} \frac{1}{T} \quad \dots\dots\dots 7.8$$

The above equation can further be rearranged as

$$\frac{1}{3} \begin{bmatrix} 2 & -1 \\ -1 & 2 \end{bmatrix} \frac{T}{I} \begin{bmatrix} n_i \\ n_j \end{bmatrix} = \frac{\|i_r(t)\|}{I} \begin{bmatrix} \sin\left(\frac{\pi}{3} - \theta\right) \\ \sin\theta \end{bmatrix} T \quad \dots\dots\dots 7.9$$

The right side of the above equation is the on-duration of the consecutive adjacent switching state vectors I_i and I_j meaning that:

$$\begin{bmatrix} t_i \\ t_j \end{bmatrix} = \frac{1}{3} \frac{T}{I} \begin{bmatrix} 2 & -1 \\ -1 & 2 \end{bmatrix} \begin{bmatrix} n_i \\ n_j \end{bmatrix} \quad \dots\dots\dots 7.10$$

The whole procedure can be summarized in the form of a block diagram as shown in Fig. 38, with the following steps:

- According to 7.4, n_k (for $k = 1, \dots, 6$) are calculated.
- The two winners n_i and n_j are selected according to the position of reference $i_r(t)$ in the sectors (for example, for $i_r(t)$ in sector II, $i = 6$ and $j = 1$).
- The on-duration t_i and t_j of the two adjacent space vectors selected in b), are obtained by performing a simple signal processing on n_i and n_j .
- The SV (switching combination, I_i and I_j) are selected by the decoder block according to the sector value.

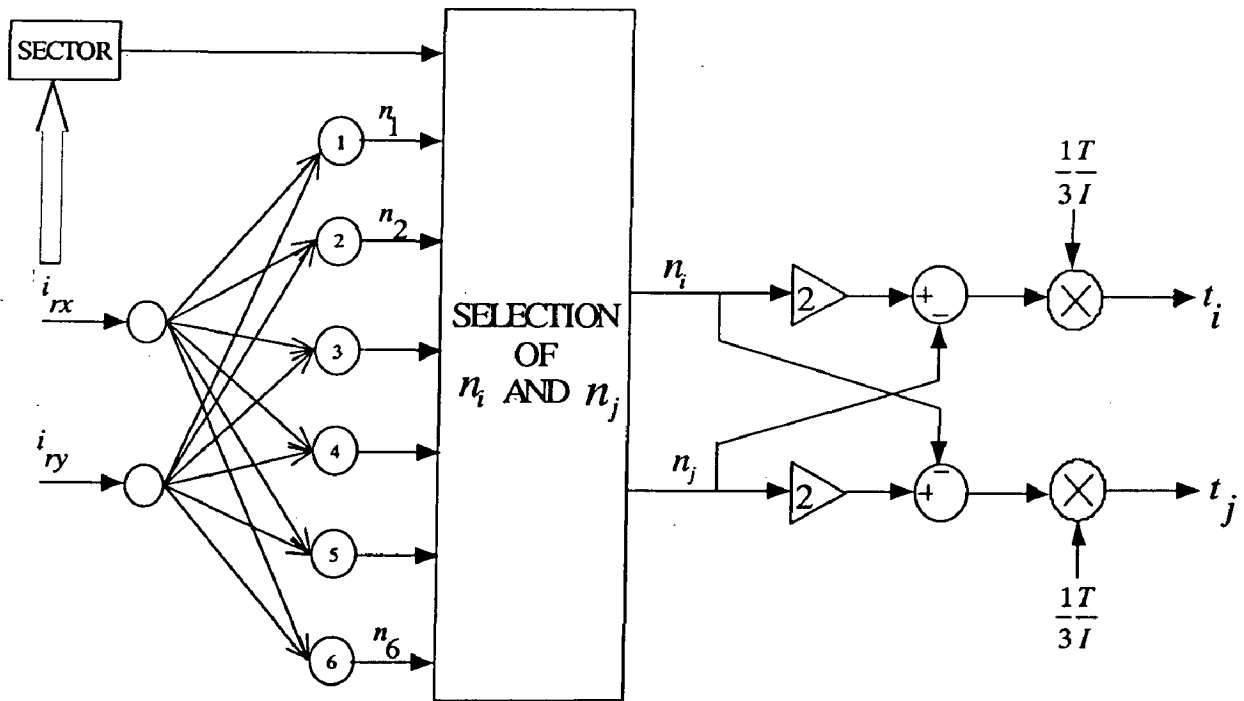


Fig. 38: Proposed SV implementation for CSAPF

When adjacent vectors and on times are determined, the procedure for defining the sequence for implementing the chosen combination is identical to that used in conventional SVM.

7.3 Modeling and Simulation Results

A model is developed with the above equations in MATLAB simulink as shown in Fig 39 and 40. The same parameters used for simulation are shown in Table II. The modulation frequency is 20 kHz. As a harmonic source a three phase diode rectifier with RL-load ($R = 64 \text{ ohm}$, $L = 10 \text{ mH}$) is used. Also, the filter inductor of 0.6 mH is used in front of the diode rectifier. Fig. 41-43 shows the simulation results of the active power filter. Total harmonic distortion (THD) of the load current is 27.80% and the total input current 3.21%.

The model is also tested with three phase diode rectifier with RC-load ($R = 64 \text{ ohm}$, $C = 1 \text{ micF}$). Fig. 44-46 shows the corresponding simulation results. Total harmonic distortion (THD) of the load current is found to be 15.34% and the total input current 2.98%.

The dynamic performance of the system is also studied under a load change from 4kW to 2kW and vice versa. It is shown in Fig. 47 and 48. It shows that the system is quite stable under sudden load change.

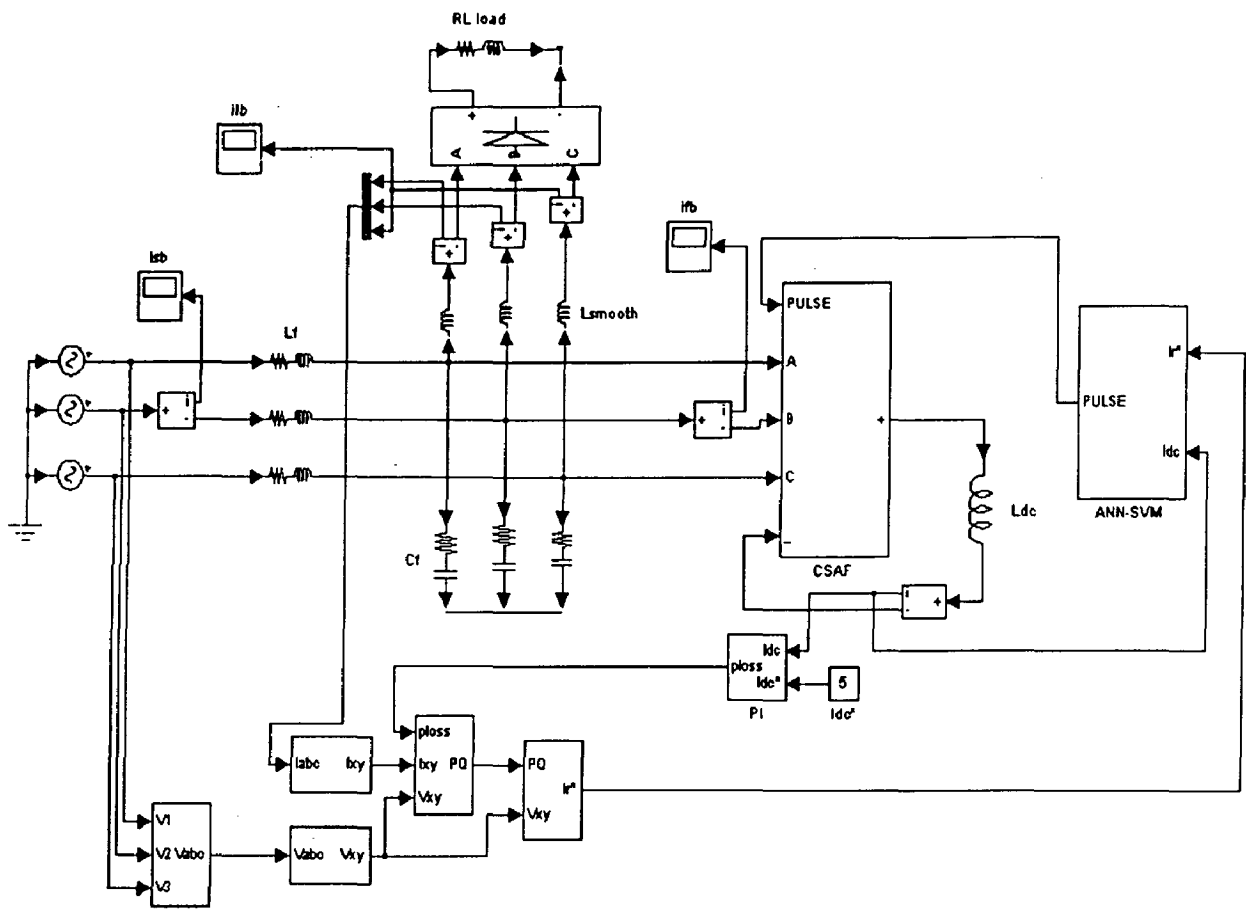


Fig 39: Simulink Model for ANN-SVM controlled CSAPF

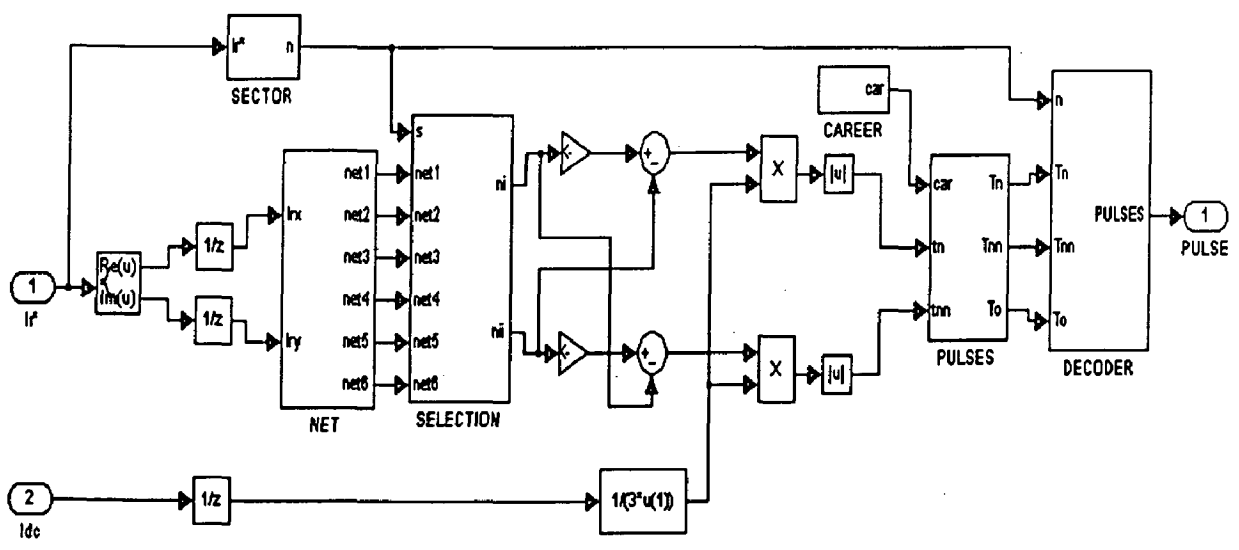


Fig. 40: Simulink Model for the Subsystem for the ANN-Space Vector Modulation

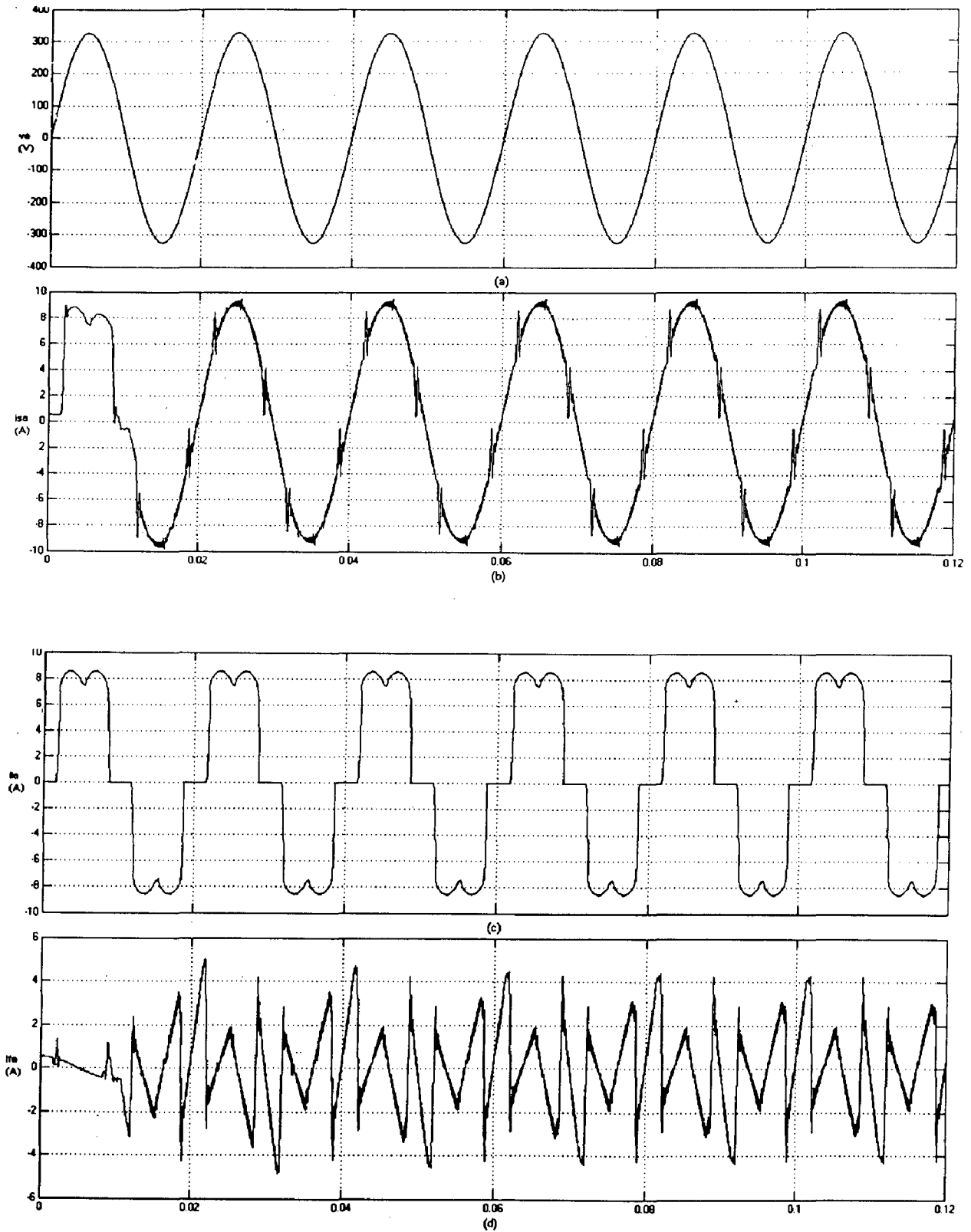


Fig. 41: (a) Source Voltage (V), (b) Source Current (A), (c) Load Current (A),
(d) Filter Current (A) for RL Load

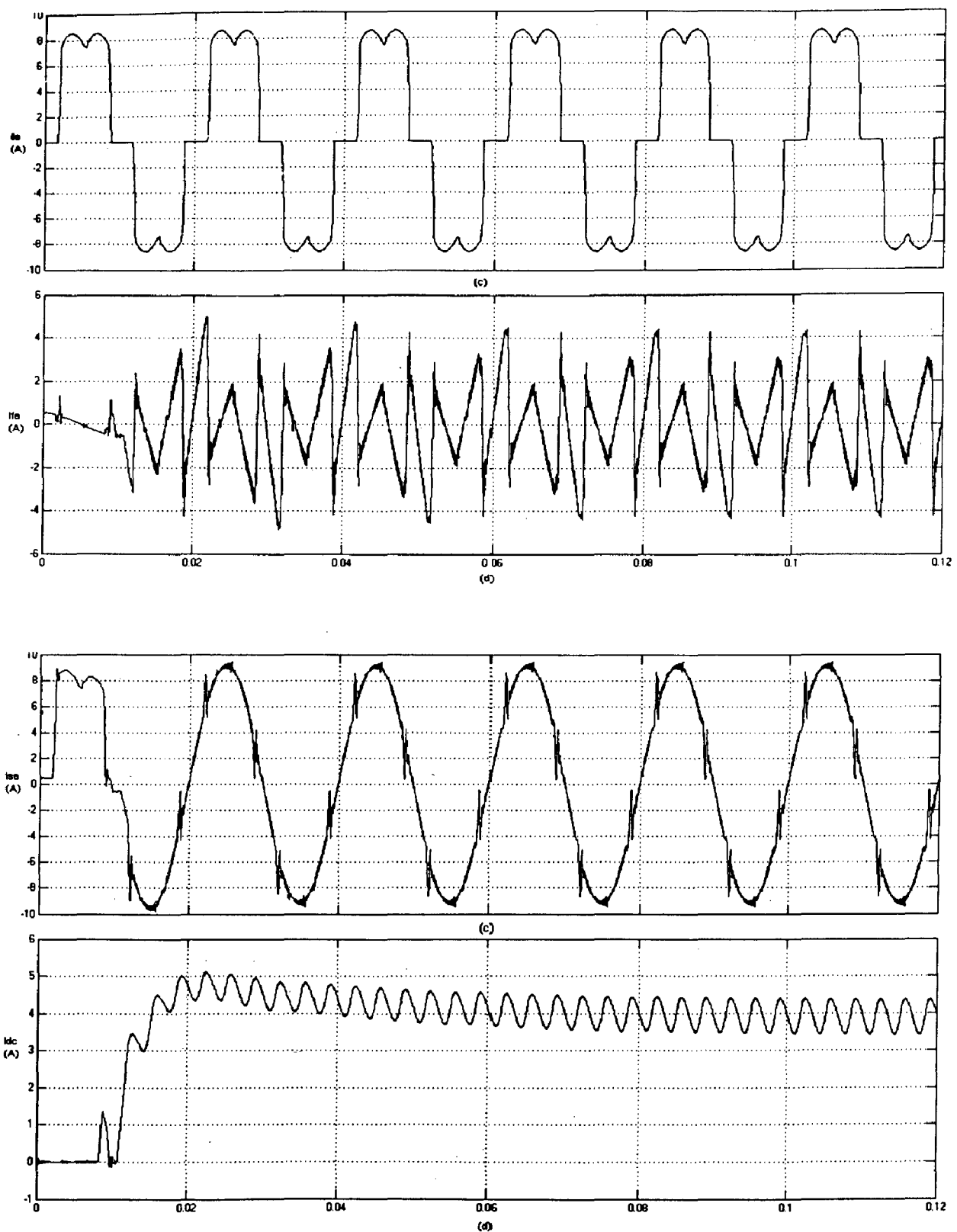


Fig. 42: (a) Load Current (A), (b) Filter Current (A), (c) Source Current (A),
 (d) DC Link Current (A) for RL Load

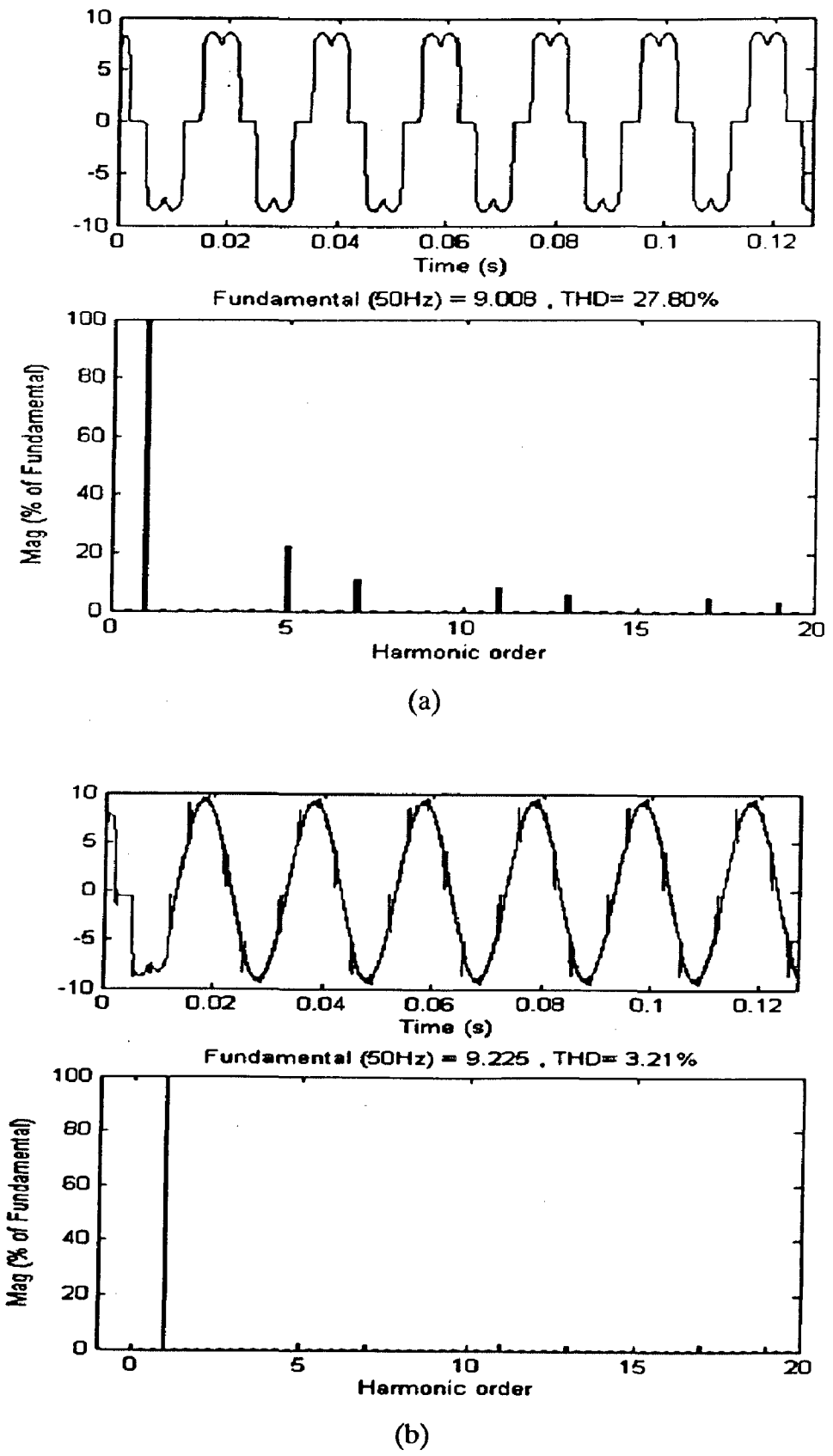


Fig. 43: FFT Analysis, (a) Load Current, (b) Source Current, for RL Load

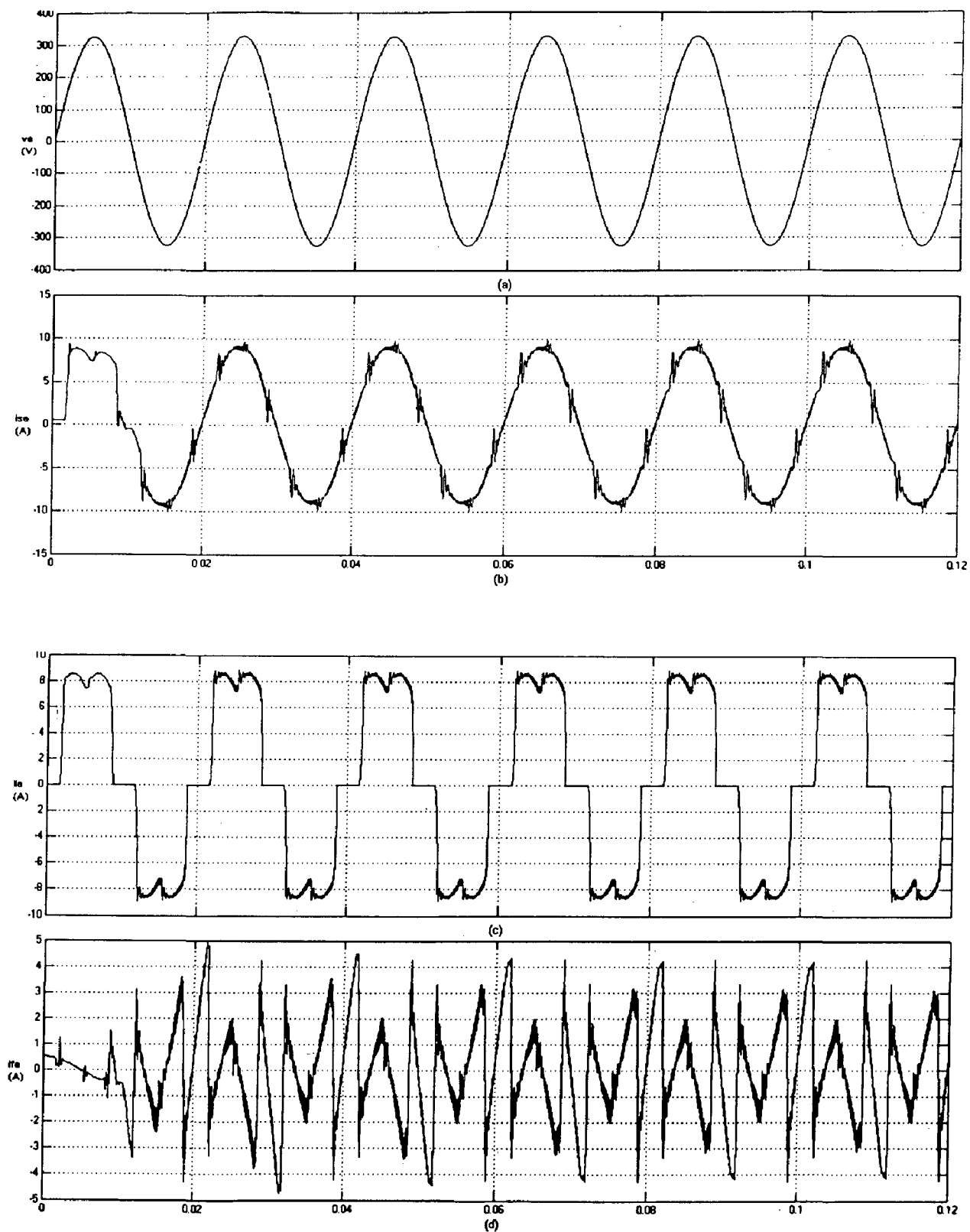


Fig. 44: (a) Source Voltage (V), (b) Source Current (A), (c) Load Current (A),
 (d) Filter Current (A) for RC Load

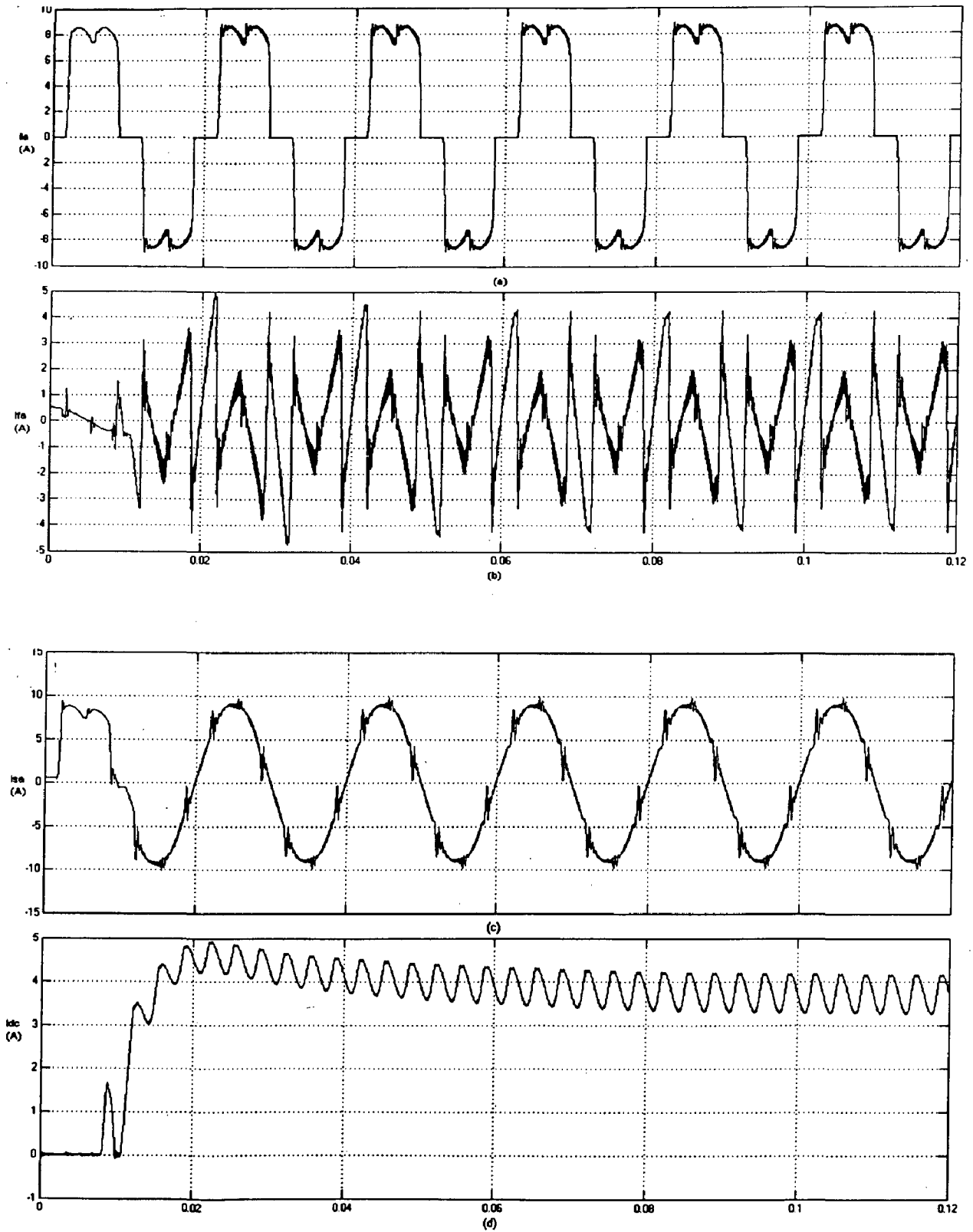
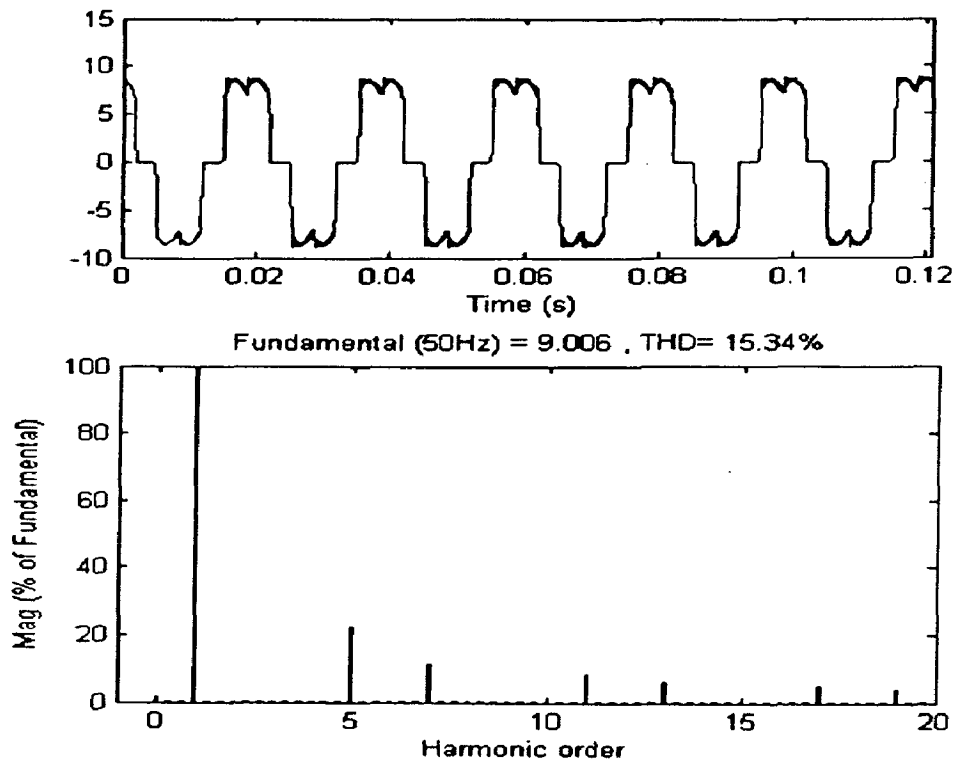
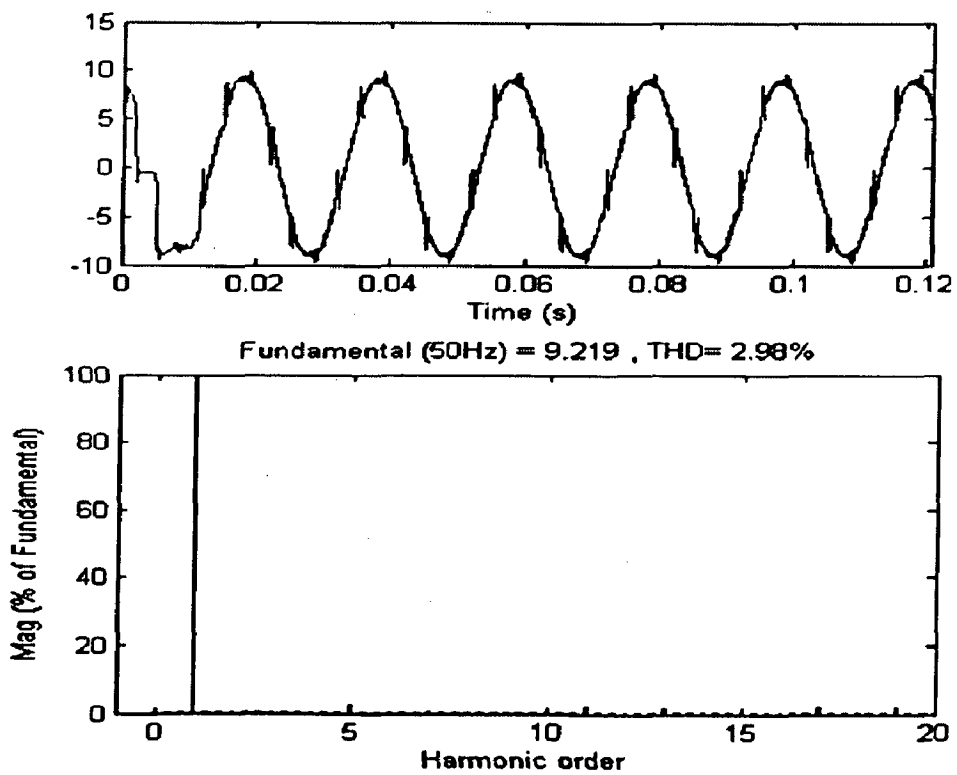


Fig. 45: (a) Load Current (A), (b) Filter Current (A), (c) Source Current (A),
(d) DC Link Current (A) for RL Load



(a)



(b)

Fig. 46: FFT Analysis, (a) Load Current, (b) Source Current, for RC Load

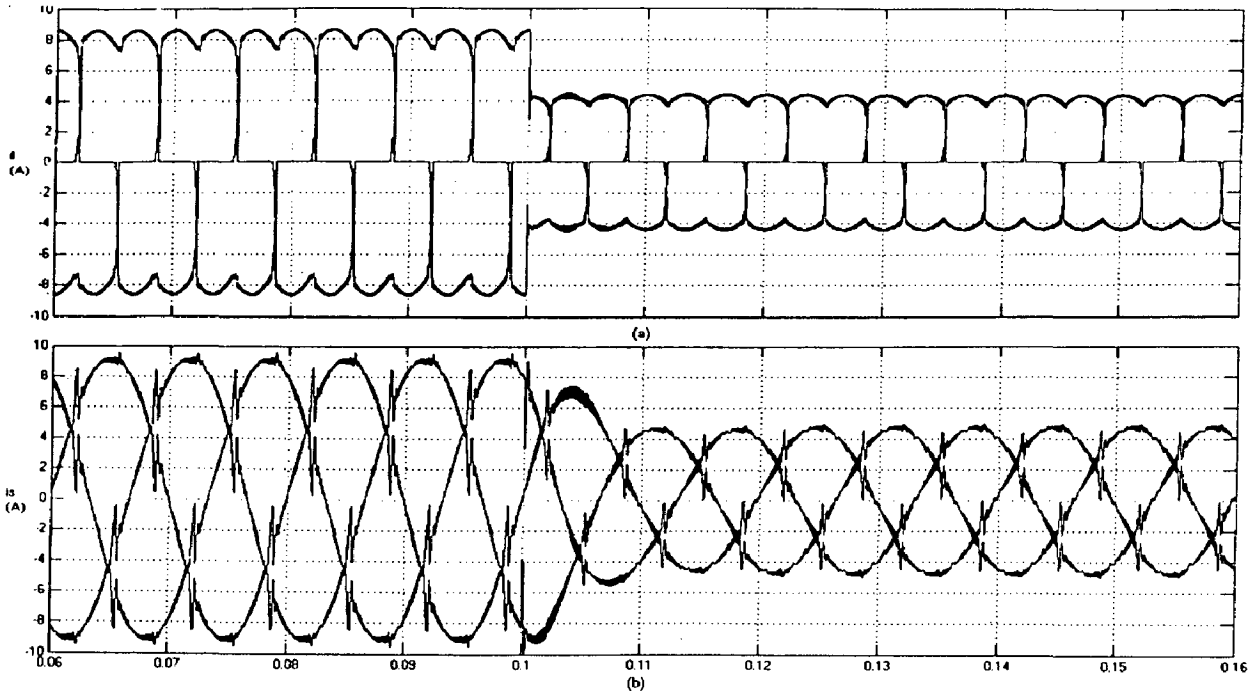


Fig. 47: Performance of AF under load change from 6.5kW to 3kW

(a) Load Current (A), (b) Source Current (A)

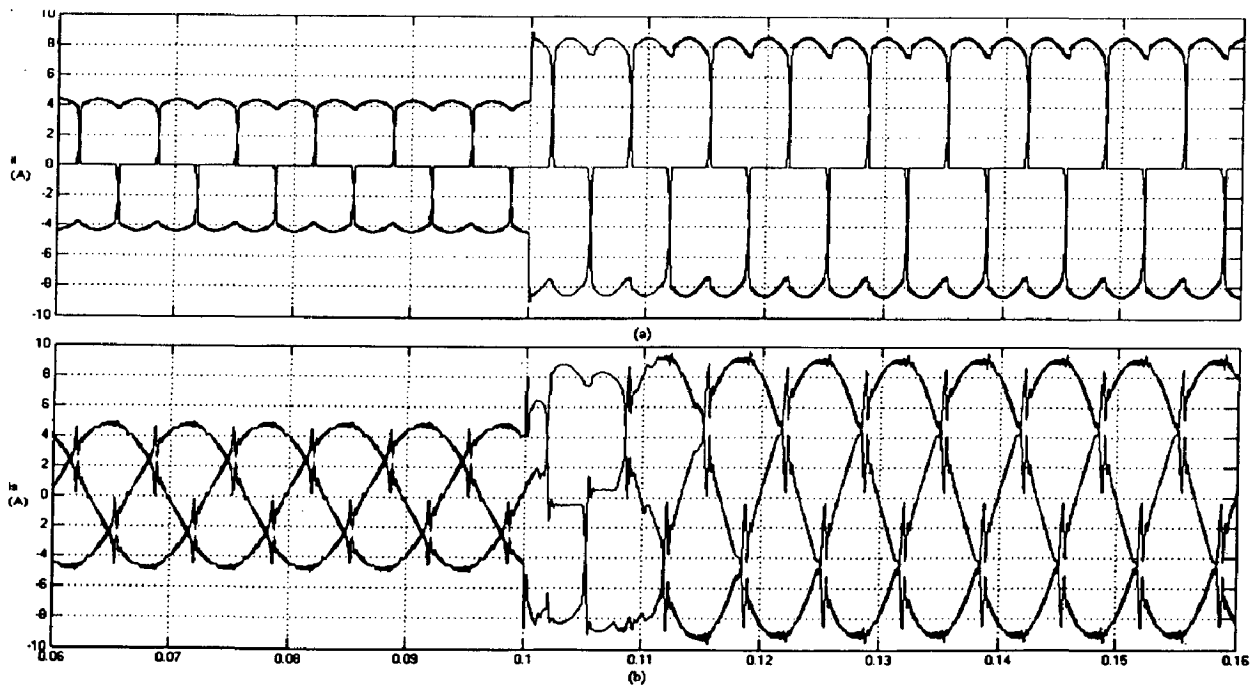


Fig. 48: Performance of AF under load change from 3kW to 6.5kW

(a) Load Current (A), (b) Source Current (A)

7.4 A Comparative Study

The Current Source Active Power Filter is implemented in three different techniques, namely the Hysteresis method, the SVM and the ANN-SVM. Simulation results of all these methods are obtained for the parameters shown in Table II with RL load ($R = 64\text{ohm}$, $L = 10\text{mH}$) and RC load ($R = 64\text{ ohm}$, $C = 1\text{micF}$) presented in subsequent chapters. The performance of an active filter is generally analyzed by comparing the THD of the source current and the load current which are presented below in tabular form.

TABLE V
Comparison of THD for different methods

| | RL LOAD | | RC LOAD | |
|--------------------|--------------|----------------|--------------|----------------|
| | Load Current | Source Current | Load Current | Source Current |
| HYSTERESIS CONTROL | 27.71% | 3.14% | 15.33% | 3.62% |
| SVM CONTROL | 27.41% | 4.64% | 15.33% | 4.14% |
| ANN-SVM CONTROL | 27.8% | 3.21% | 15.34% | 2.98% |

The results show that the ANN SVM approach, having the advantage of lesser switching losses performs quite comparably with hysteresis control. With compared to conventional SVM, the ANN-SVM gives better performance with faster execution and capacity to operate at much higher modulation frequencies.

CHAPTER-8

CONCLUSION AND FUTURE SCOPE

In this paper different PWM technique for implementation of a Current Source based Power Filters are presented. Among the various PWM techniques, the hysteresis band current control is used very often because of its simplicity of implementation. Also, besides fast response current loop, the method does not need any knowledge of load parameters. Though it gives much reduced THD for source current (in range of 3%), the current control with a fixed hysteresis band has the disadvantage that the PWM frequency varies within a band because peak-to-peak current ripple is required to be controlled at all points of the fundamental frequency wave. Also it consumes much power due to high switching loss which can be confirmed by comparing the in-phase fundamental components of source current and load current. Also there is considerable amount of parasitic harmonics in PWM waveforms.

The superior characteristics of the SVM technique is that number of switching are 30 percent less than those obtained by hysteresis PWM. In balanced three phase three wire system, the sum of instantaneous three phase current must be zero. This means that the current of one phase depends on the state of the other. In the space vector modulation (SVM) technique, this relation is implied in the state space vectors. The main drawback of this system is that it uses nonlinear trigonometric functions which makes it more complex for implementation and it takes more execution time. Use of look-up tables for such functions introduces an execution error and requires much memory space.

This paper presents an alternative SVM implementation that is based on a neural network structure and its classification properties. Neural networks are effectible implemented for decoupling and linearising the conventional SVM. The technique reduces software complexity, computation time, and increases the accuracy of the positioning of the switching instants. It uses simple signal processing and no look-up table. The following characteristics are therefore improved: (a) possibility of higher switching frequencies, (b) higher bandwidth for the control loops, (c) reduced software, and (d) reduction of parasitic harmonics in PWM waveforms.

The work can be further extended by including the estimation of harmonics by an adaptive network. A new approach of adaptive estimation of harmonics by Fourier linear combiner can be realized using linear adaptive neural network, called ADALINE. It has an input sequence, an output sequence, and a desired response sequence signal. The weight vectors, which can be adjusted by Widro-Hoff delta rule, generate the Fourier coefficients of the signal. Thus a totally adaptive and linear line conditioning system can be developed by combining the ADALINE harmonic estimation and the ANN-SVM implementation for CSAPF.

References

- [1] A. Ghosh and G. Ledwich, "Power Quality Enhancement Using Custom Power Devices," Kluwer Academic Publishers Boston 2002.
- [2] H. Rudnick, J. Dixon and L. Morán, "Active Power Filter as a solution to power quality problems in distribution network," IEEE power & energy magazine, september, 2003.
- [3] S.M. Williams and R.G. Hoft, "Implementation of current source inverter for power line conditioning," IEEE Trans. 1990.
- [4] B. Singh, K. Al Haddad and A. Chandra, "A New Control Approach to Three-phase Active Filter for Harmonics and Reactive Power Compensation", IEEE Trans. 1997.
- [5] M. Milosevic, "Hysteresis Current Control in Three-Phase Voltage Source Inverter"
- [6] D. Graovac, V. Kati, A. Rufer and J. Kne, "Unified power quality conditioner based on Current Source Converter topology" , EPE 2001.
- [7] E.H. Song, B.K. Kwon, "A Novel Digital Control for Active Power Filters", IEEE 1992.
- [8] M. Salo and H. Tuusa, "A New Control Method for a Current-Source Active Power Filter", IEEE 2000

- [9] B.H. Kown, B. Min, "A Fully Software-Controlled PWM Rectifier with Current Link", IEEE Trans. 1993
- [10] M. Routimo, M. Salo, H. Tuusa, "Comparison of Voltage-Source and Current-Source Shunt Active Power Filters", IEEE 2005
- [11] N.R. Zargari, G. Joos, P.D. Ziogas, "Input Filter Design for PWM Current Source Rectifiers", IEEE 1993
- [12] A. Bakhshai, J. Espinoza, G. Joos, H. Jin, "A Combined Artificial Neural Network and DSP approach to the implementation of Space Vector Modulation Techniques"
- [13] M. Salo, "AC Current Sensorless Control of the Current-Source Active Power Filter", IEEE 2005.